

# Source apportionment of single particles sampled at the industrially polluted town of Port Talbot, United Kingdom by ATOFMS

Taiwo, Adewale M.; Harrison, Roy M.; Beddows, David C.s.; Shi, Zongbo

DOI:

[10.1016/j.atmosenv.2014.08.009](https://doi.org/10.1016/j.atmosenv.2014.08.009)

License:

Other (please specify with Rights Statement)

Document Version

Peer reviewed version

Citation for published version (Harvard):

Taiwo, AM, Harrison, RM, Beddows, DCS & Shi, Z 2014, 'Source apportionment of single particles sampled at the industrially polluted town of Port Talbot, United Kingdom by ATOFMS', *Atmospheric Environment*, vol. 97, pp. 155-165. <https://doi.org/10.1016/j.atmosenv.2014.08.009>

[Link to publication on Research at Birmingham portal](#)

## Publisher Rights Statement:

NOTICE: this is the author's version of a work that was accepted for publication in *Atmospheric Environment*. Changes resulting from the publishing process, such as peer review, editing, corrections, structural formatting, and other quality control mechanisms may not be reflected in this document. Changes may have been made to this work since it was submitted for publication. A definitive version was subsequently published in *Atmospheric Environment*, Volume 97, November 2014, Pages 155–165 DOI: 10.1016/j.atmosenv.2014.08.009  
Checked for repository 30/10/2014

## General rights

Unless a licence is specified above, all rights (including copyright and moral rights) in this document are retained by the authors and/or the copyright holders. The express permission of the copyright holder must be obtained for any use of this material other than for purposes permitted by law.

- Users may freely distribute the URL that is used to identify this publication.
- Users may download and/or print one copy of the publication from the University of Birmingham research portal for the purpose of private study or non-commercial research.
- User may use extracts from the document in line with the concept of 'fair dealing' under the Copyright, Designs and Patents Act 1988 (?)
- Users may not further distribute the material nor use it for the purposes of commercial gain.

Where a licence is displayed above, please note the terms and conditions of the licence govern your use of this document.

When citing, please reference the published version.

## Take down policy

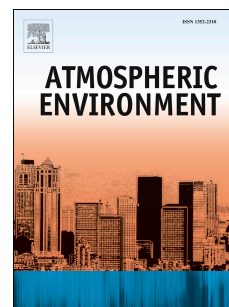
While the University of Birmingham exercises care and attention in making items available there are rare occasions when an item has been uploaded in error or has been deemed to be commercially or otherwise sensitive.

If you believe that this is the case for this document, please contact [UBIRA@lists.bham.ac.uk](mailto:UBIRA@lists.bham.ac.uk) providing details and we will remove access to the work immediately and investigate.

# Accepted Manuscript

Source Apportionment Of Single Particles Sampled At The Industrially Polluted Town Of Port Talbot, United Kingdom BY ATOFMS

Adewale M. Taiwo, Roy M. Harrison, David C.S. Beddows, Zongbo Shi



PII: S1352-2310(14)00603-7

DOI: [10.1016/j.atmosenv.2014.08.009](https://doi.org/10.1016/j.atmosenv.2014.08.009)

Reference: AEA 13160

To appear in: *Atmospheric Environment*

Received Date: 11 March 2014

Revised Date: 28 July 2014

Accepted Date: 4 August 2014

Please cite this article as: Taiwo, A.M., Harrison, R.M., Beddows, D.C.S., Shi, Z., Source Apportionment Of Single Particles Sampled At The Industrially Polluted Town Of Port Talbot, United Kingdom BY ATOFMS, *Atmospheric Environment* (2014), doi: 10.1016/j.atmosenv.2014.08.009.

This is a PDF file of an unedited manuscript that has been accepted for publication. As a service to our customers we are providing this early version of the manuscript. The manuscript will undergo copyediting, typesetting, and review of the resulting proof before it is published in its final form. Please note that during the production process errors may be discovered which could affect the content, and all legal disclaimers that apply to the journal pertain.

**SOURCE APPORTIONMENT OF SINGLE PARTICLES  
SAMPLED AT THE INDUSTRIALLY POLLUTED  
TOWN OF PORT TALBOT, UNITED KINGDOM  
BY ATOFMS**

**Adewale M. Taiwo, Roy M. Harrison<sup>\*1</sup>, David C.S. Beddows  
and Zongbo Shi**

**Division of Environmental Health Risk Management  
School of Geography, Earth & Environmental Sciences  
University of Birmingham  
Edgbaston, Birmingham, B15 2TT  
United Kingdom**

---

<sup>\*</sup> To whom correspondence should be addressed

Tele: +44 121 414 3494; Fax: +44 121 414 3708; Email: r.m.harrison@bham.ac.uk

<sup>1</sup> Also at: Department of Environmental Sciences / Center of Excellence in Environmental Studies, King Abdulaziz University, Jeddah, 21589, Saudi Arabia

**ABSTRACT**

Single particle analysis of an industrially polluted atmosphere in Port Talbot, South Wales, United Kingdom was conducted using Aerosol-Time-of-Flight Mass Spectrometry (ATOFMS). During the four week sampling campaign, a total of 5,162,018 particles were sized in the size range 0.2 to 1.9  $\mu\text{m}$  aerodynamic diameter. Of these, 580,798 were successfully ionized generating mass spectra. K-means clustering employed for analysing ATOFMS data utilized 96% of the hit particles to generate 20 clusters. Similar clusters were merged together and 17 clusters were generated from which 7 main particle groups were identified. The particle classes include: K-rich particles (K-CN, K-NO<sub>3</sub>, K-EC, K-Cl-PO<sub>3</sub> and K-HSO<sub>4</sub>), aged sea salt (Na-NO<sub>3</sub>), silicate dust (Na-HSiO<sub>2</sub>), sulphate rich particles (K-HSO<sub>4</sub>), nitrate rich particles (AlO-NO<sub>3</sub>), Ca particles (Ca-NO<sub>3</sub>), carbon-rich particles (Mn-OC, Metallic-EC, EC, EC-NO<sub>3</sub> and OC-EC), and aromatic hydrocarbon particles (Arom-CN, Fe-PAH-NO<sub>3</sub> and PAH-CN). With the aid of wind sector plots, the K-Cl-PO<sub>3</sub> and Na-HSiO<sub>2</sub> particle clusters were related to the steelworks blast furnace/sinter plant while Ca-rich particles arose from blast furnace emissions. K-CN, K-EC, Na-HSiO<sub>2</sub>, K-HSO<sub>4</sub>, Mn-OC, Arom-CN, Fe-PAH-NO<sub>3</sub>, and PAH-CN particles were closely linked with emissions from the cokemaking and mills (hot and cold) steelworks sections. Na-HSiO<sub>2</sub> particles were also associated with the blast furnace and crustal matter. The source factors identified by the ATOFMS were compared with those derived from multivariate analysis using Multilinear Engine (ME-2) applied to filter samples analysed off-line. Both methods of source apportionment identified common source factors including those within the steelworks (blast furnace, sinter, cokemaking), as well as marine, traffic and secondary particles, but quantitative attribution of mass is very different.

**Keywords:**

Single particle; steelworks; wind sector; source contribution; ME-2; ATOFMS

## 1. INTRODUCTION

Aerosol Time-of-Flight Mass Spectrometry (ATOFMS) provides continuous, real-time detection and characterization of single particles from polydisperse samples, supplying information on particle size and composition. (Gross et al., 2000; Gard et al., 1997; Prather et al., 1994). It is a technique well suited to determine the size and composition of large numbers of particles (Sullivan and Prather, 2005). The advantage of ATOFMS over other methods of source apportionment is its ability to identify associations among chemical species within individual particles. This association can be related directly to source apportionment (Kelly et al., 2003). However, the key disadvantages are the cost of instrument purchase, and interpretation of the spectra which requires a steep learning curve (Kelly et al., 2003). The deployment of ATOFMS for both outdoor and indoor pollution studies has been widely reported in published work (Held et al., 2002; Dall'Osto et al., 2004; 2007; 2008; 2012; Gross et al., 2000; Healy et al., 2013; Smyth et al., 2013). Despite the numerous studies conducted around the world on single particle measurement, only a few have been carried out in the vicinity of steel industries (Dall'Osto et al., 2008; 2012).

The ATOFMS instrument has proved its ability to resolve particles in emissions associated with different fuel-types. In Northern Mexico City, Moffet et al. (2008) were able to measure ambient aerosol in the industrial and residential areas of the city using ATOFMS. Their findings indicated that biomass burning and industrial emissions made significant contributions to primary particle loadings in Mexico City, exhibiting strong correlations with local meteorology. Results also showed that the majority of particles in the submicrometre range comprised emissions from biomass/biofuel burning (40%) and aged organic carbon (31%), internally mixed with oxidized OC ( $C_2H_3O$ ,  $m/z = 43$ ), nitrate, sulphate and ammonium. The study demonstrated the value of the ATOFMS as a tool for identifying biomass markers and also for the apportionment of particulate matter.

Dall'Osto and Harrison (2006) employed the ATOFMS instrument for single particle analysis of PM in Athens (Greece). A unique 'car particle' due to signals at  $m/z$  54 ( $^{54}\text{[Fe]}^+$ ), 56 ( $^{56}\text{[Fe]}^+$ ), 88  $[\text{FeO}_2]^+$ , 138  $[\text{Ba}]^+$  and 154  $[\text{BaO}]^+$  was identified as a traffic fingerprint. Five broad classes of PM identified during the study were sea salt, dust, carbon, inorganic and K-rich particles. Secondary carbonaceous particles which could have been difficult to detect by other means were also revealed in the study. Sullivan et al. (2007) also adopted ATOFMS for online characterization of the composition of particles from the marine environment. ART-2a software used for classification of particles showed that nitrate and sulphate made up 60-80% of PM in the super-micrometre size range. The observed nitrate and sulphate were associated with mineral dust particles emitted during dust events. Giorio et al. (2012) applied three different techniques to analyse ATOFMS data collected in London, UK. The data analysis techniques used were PMF, ART2a and k-means clustering (in the ENCHILADA package). Among the components revealed by ATOFMS were fresh and aged EC, organics, sodium chloride, sulphate, nitrogen and potassium. This showed that the ATOFMS is capable of identifying aged and freshly emitted particles. With an ATOFMS instrument, Smyth et al. (2013) in their recent study at a sampling site in Milwaukee, USA attributed emissions of Se, Cd, Sb and Mo to a coal-fired plant. Bromine containing compounds that could have been difficult to determine with offline instrumentation were also revealed by ATOFMS.

Studies involving source apportionment of single particles have been reported in several published works (i.e. Owega et al., 2004; Bein et al., 2006; 2007; Reinard et al., 2007; Eatough et al., 2008; Snyder et al., 2010; Ault et al., 2010; Healy et al., 2009; 2011; McGuire et al., 2011). For instance, Eatough et al. (2008) has applied a Positive Matrix Factorization (PMF) model to identify and apportion single particles collected in Riverside, US. Sources identified were diesel, secondary nitrate, ozone-related secondary aerosol, basin transported source and organic emissions. The PMF model was also applied to filter-based measurements. Source apportionment of the two types of

measurements were consistent in the identification of emission sources in the study area. A related study by Snyder et al. (2010) identified metals including Ca, Co, Fe, Pb, Ni, K and Zn in single particles collected in East St. Louis, Illinois, US. These metals were closely linked to sources such as: petroleum refineries, power plants, cement kiln, and waste incinerator. High loadings of Sb, Ba, Cd and Se were found for the power plant. Application of PMF to single particles has also been reported in a study conducted in Toronto, Canada (Owega et al., 2004). Sources identified were biogenic, crustal, organic nitrate, construction dust, soil/road salt, secondary salt, wood burning, inter-continental dust and an aluminium-fluoride source. The study by Ault et al. (2010) has identified a unique plume particle (OC-V-Sulphate- that represented a 10-34% source contribution) in the port of Los Angeles, US.

In the present study an ATOFMS instrument was used alongside filter-based samplers and continuous analysers in a campaign-based study of a steelworks in South Wales, UK. An analysis of particle size distributions has already been reported (Taiwo et al., 2014a), as has a receptor modelling study with the Multi-linear Engine, ME-2 model (Taiwo et al., 2014b).

## **2. MATERIALS AND METHODS**

### **2.1 The Study Area**

Port Talbot (PT) is a coastal industrial town with a population of approximately 35,000, located in South Wales (51° 34' N and 3° 46' W). The Tata steelworks complex located in Port Talbot is the main industry in the study area and a major source of PM emissions (AQEG, 2011). The site covers approximately 28 km<sup>2</sup>, contains ~50 km of roads, 100 km of railway, and has 25,000 vehicle movements per day. The production capacity is around 5 million tonnes per year with the main processes in the steelworks being iron-making (sintering, blast furnace and raw materials), steel-making (basic oxygen steel-making (BOS) and coking) and rolling mills (hot and cold mills)

(Moreno et al., 2004; Dall'Osto et al., 2008). Figure 1 shows the sampling site (Fire Station) in Port Talbot where the ATOFMS instrument was located.

## 2.2 Aerosol Sampling and Instrumentation

Single particle sampling during the four-week campaign (April 18-May 16, 2012) at Port Talbot was carried out using the TSI ATOFMS (Model 3800-100 fitted with an aerodynamic lens inlet). The ATOFMS instrumentation has been well described by Gard et al. (1997). Particles passing the aerodynamic lens are accelerated into a vacuum, their transit time between two low powered lasers giving a measure of particle size. The particles are then ionised by a Nd:YAG laser at 266 nm, the ionised fragments entering positive and negative time-of-flight mass spectrometers. Size calibration was achieved by ranges of polystyrene latex spheres (PSL) in the diameter range 0.1-1.3  $\mu\text{m}$ . These were introduced from a medical atomizer. Mass-to-charge ( $m/z$ ) calibration was done with NaCl and graphite powder. A solution containing Li, Na, K and Pb was also introduced for mass calibration. Upon calibration, the data is loaded into the MS Analyse program to obtain a better fit curve for both size and mass.

During the four week campaign, 5,162,018 particles were sized of which 580,798 were successfully ionized (hit particles). Successfully ionized particles were imported into the ENCHILADA software (Gross et al., 2000; Giorio et al., 2012) for analysis.

Size distribution of ATOFMS counts were scaled with Grimm optical particle (model 1.108) counter operated simultaneously with the ATOFMS instrument at the same sampling site (Fire Station). The Grimm data was used for inlet efficiency (inverse transmission efficiency,  $E$ ) calibration. The scaling is spread across the entire ATOFMS data generated during the campaign. Inverse transmission efficiency,  $E$  is calculated therefore as:



$$E = N_{\text{Grimm}}/N_{\text{ATOFMS}}$$

where,  $N_{\text{Grimm}}$  is the Grimm particle number concentration,  $N_{\text{ATOFMS}}$  is ATOFMS particle number concentration. ATOFMS particles are defined by number counts of total hit and missed particles that correspond to same size range as the Grimm particle counter. The size range of ATOFMS particles during the campaign is 0.2-1.9  $\mu\text{m}$  while the total size range of the Grimm was 0.3-20  $\mu\text{m}$ . The particle sizes where E was calculated to fit with the Grimm size range are in the intervals 0.3-0.4, 0.4-0.5, 0.5-0.65, 0.65-0.8, 0.8, 1.0, 1.0-1.6 and 1.6-2.0  $\mu\text{m}$ . The inverse transmission efficiency curve follows an inverse power law pattern within the particle diameter range of 0.39-1.8  $\mu\text{m}$ , in line with the findings of Dall'Osto et al. (2006).

Mass concentrations of the particle clusters were calculated from the scaled ATOFMS particle counts assuming spherical geometry and a density depending on the particle type. In the published literature, some authors have used a common particle density value to quantify the single particle mass (Prather, 1998; Healy et al., 2013). In this study, we adopted different density values to calculate mass concentrations because PM in Port Talbot is influenced by multiple factors including the steelworks, sea salt, crustal, traffic and long range transportation (AQEG, 2011). These values were selected from the published work of Phillips and Perry (1995) and Chemical Book (2008). The values of particle density were 1.55  $\text{g cm}^{-3}$  for K-CN, 2.11  $\text{g cm}^{-3}$  for K- $\text{NO}_3$ , 2.56  $\text{g cm}^{-3}$  for K- $\text{Cl-PO}_4$ , 2.26  $\text{g cm}^{-3}$  for Na- $\text{NO}_3$ , 2.61  $\text{g cm}^{-3}$  for silica dust, 2.66  $\text{g cm}^{-3}$  for K- $\text{HSO}_4$ , 1.72  $\text{g cm}^{-3}$  for AlO- $\text{NO}_3$ , 2.50  $\text{g cm}^{-3}$  for Ca- $\text{NO}_3$ , 2.1  $\text{g cm}^{-3}$  for EC or black carbon, 6.89  $\text{g cm}^{-3}$  for Mn-OC and 5.0  $\text{g cm}^{-3}$  for Fe-PAH- $\text{NO}_3$ . The densities of aromatic and polyaromatic hydrocarbons were obtained from Mackay et al. (2006) as 0.78 and 1.27  $\text{g cm}^{-3}$  respectively. The value of OC was also taken as 1.40  $\text{g cm}^{-3}$  (Gysel et al., 2007).

### 3. RESULTS AND DISCUSSION

#### 3.1 ATOFMS Chemical Composition

The chemically analysed (hit particles) represented 11.2% of the total sampled particles. Out of the total ionized particles, ENCHILADA utilised 96% (555,798 particles) in a k-means clustering program to generate 20 clusters which were reduced to 17 clusters (by merging similar clusters with related spectral peaks and diurnal or temporal variations). The scaled mean diameters as well as percentages represented by these particle clusters are reported in the Supplementary Information, Table S1. Most of the particle classes defined by the clusters exhibited mean particle diameter ( $D_p$ ) less than  $1.0\ \mu\text{m}$  (scaled mean diameter), except  $\text{Na-NO}_3$ , which occurred at  $D_p > 1.0\ \mu\text{m}$ . These clusters were categorized as: (1) K-rich particles which comprised **K-CN, K-NO<sub>3</sub>, K-EC, K-Cl-PO<sub>3</sub>, and K-HSO<sub>4</sub>** classes, (2) Silicate Dust, **Na-HSiO<sub>2</sub>**, (3) Ca-rich particles, **Ca-NO<sub>3</sub>**, (4) Carbon-rich particles, **Mn-OC, Metallic-EC, EC and OC-EC** and (5) Aromatic Hydrocarbon (Arom) and PAH particles, **Arom-CN, Fe-PAH-NO<sub>3</sub> and PAH-CN**, (6) Aged Sea Salt, **Na-NO<sub>3</sub>**, and (7) Al Nitrate-rich particles, **AlO-NO<sub>3</sub>**. The mean mass spectra of all the particle clusters identified are shown in Figure 2. The polar plots of individual particle types that are related to the steelworks emissions are shown in Figure 3, while other polar plots are depicted in Figure S1 in the Supplementary Information. The polar plots show particle abundance as a function of wind direction (angle from centre) and wind speed (distance from centre of plot) and are a valuable aid to identifying particle sources.

##### 3.1.1 K-rich particle types

This category includes K-CN, K-NO<sub>3</sub>, K-EC, K-Cl-PO<sub>3</sub>, and K-HSO<sub>4</sub>, and comprised 40% of the total ionized particles. The high abundance of the K-rich particles is partially explained by the extreme sensitivity of the ATOFMS instrument to K (Healy et al., 2013).

The **K-CN particle** class is characterised by an elevated positive ion signal at  $m/z +39$   $[K]^+$  and intense negative signal at  $m/z -26$   $[CN]^-$ . Other weaker peaks are found at  $m/z +23$   $[Na]^+$ ,  $m/z -46$   $[NO_2]^-$ ,  $m/z -62$   $[NO_3]^-$ ,  $m/z -97$   $[HSO_4]^-$ ,  $m/z -35$   $[Cl]^-$ ,  $m/z -42$   $[CNO]^-$ ,  $m/z -48$   $[C_4]^-$ ,  $m/z -60$   $[C_5]^-$  and  $m/z -72$   $[C_6]^-$ . The polar plot shows multiple source areas for this particle class suggesting much influence from diffuse local sources (Figure 3). Evidence for a steelworks contribution can be seen in the elevated concentration of the cluster towards the south-easterly and southerly wind-direction. The mills (hot and cold) and cokemaking units of Port Talbot steelworks are located in the 150-190° wind sector. Table 1 shows the wind sectors linking different steelworks processes with the Fire Station monitoring site where the ATOFMS instrument was located. Contributions from the steelmaking section were indicated for this particle type. K is a notable biomass burning/woodsmoke marker but has also been reported from the steelworks sinter plant (Hleis et al., 2013). An ATOFMS K-CN particle sampled in Athens, Greece, by Dall'Osto and Harrison (2006) was attributed to vegetative debris. The  $[CN]^-$  ion, as suggested by Tao et al. (2011), might not necessarily indicate the presence of cyanide but of carbon and nitrogen within an organic particle. In this study the  $CN^-$  ion may have an origin in cokemaking emissions. Wastewater from cokemaking at the steelworks has been reported to contain significant amount of cyanide and thiocyanate ([http://www1.eere.energy.gov/manufacturing/resources/steel/pdfs/roadmap\\_chap4.pdf](http://www1.eere.energy.gov/manufacturing/resources/steel/pdfs/roadmap_chap4.pdf)).

The **K-NO<sub>3</sub> particle** class showed strong peaks for potassium ( $m/z +39$ ) and  $NO_2^-$  and  $NO_3^-$  ( $m/z -46$  and  $-62$ ). Smaller peaks were also present for  $[CN]^-$  ( $m/z -26$ ),  $[Cl]^-$  ( $m/z -35$ ), and  $[HSO_4]^-$  ( $m/z -97$ ). The polar plot reveals that the origin of K-NO<sub>3</sub> particles is located to the north of the sampling site. This may be related to traffic emissions from the major roads as well as residential woodsmoke (see Port Talbot map in Figure 1).

226 The **K-EC particle** class shows strong peaks for potassium ( $m/z +39$ ) and elemental carbon, EC  
 227 ( $m/z [C_n]^-$ ,  $n=2-9$ ). Smaller peaks from nitrite and nitrate ( $m/z -46$  and  $-62$ ), sodium ( $m/z +23$ ) and  
 228  $[C_5]^+$  ( $m/z +60$ ) are also observed in this class. The polar plots of the K-EC and K-CN clusters are  
 229 very similar suggesting a common emission source type. However, the temporal correlation  
 230 between the two clusters is weak ( $r^2 = 0.13$ ). K is a widely used tracer of woodsmoke while EC is  
 231 emitted from traffic and coal combustion (Dan et al., 2004; Harrison et al., 2012a) as well as in  
 232 woodsmoke. The wind sector plot (Figure 3) suggests contributions from the mills (cold and hot) as  
 233 the largest emitter of K-EC particles. Possible emissions from the cokemaking ovens and residential  
 234 combustion to the north and west are also suggested by the polar plot. The earlier work at Port  
 235 Talbot did not report the K-EC particle (Dall'Osto et al., 2012). This particle type was however  
 236 reported by Healy et al. (2013) at an urban background site in Paris and was attributed to local  
 237 biomass combustion. The study of Bi et al. (2011) in the Pearl River Delta urban area also attributed  
 238 this particle type to biomass combustion.

240 The **K-Cl-PO<sub>3</sub> particle** class is characterized by strong peaks observed at  $m/z 39 [K]^+$ ,  $m/z -35$   
 241  $[Cl]^-$ ,  $m/z -79 [PO_3]^-$  and  $m/z -96 [HPO_3]^-$ . Possible sources are the sinter plant or biomass burning  
 242 (Li et al., 2003; Dall'Osto et al., 2008, Hleis et al., 2013). The recent work of Hleis et al. (2013) has  
 243 reported KCl as a good indicator of sinter plant emissions. The polar plot also established the sinter  
 244 plant (located between  $190-270^\circ$  of the sampling site, Table 1) as the most likely source. The source  
 245 of phosphate is unknown. The study by Dall'Osto et al. (2008) linked phosphate emissions to the  
 246 rolling mills which is not consistent with the wind sector polar plot in this study.

#### 248 **K-HSO<sub>4</sub> particle type**

249 The sulphate-rich particle class is characterised by an elevated negative peak of  $m/z -97 [HSO_4]^-$   
 250 plus other weak peaks at  $m/z -26 [CN]^-$ ,  $-46 [NO_2]^-$ ,  $-62 [NO_3]^-$  and  $-80 [SO_3]^-$ . The positive  
 251 spectrum is dominated by the presence of  $m/z +39 [K]^+$  and other smaller peaks at  $m/z +23 [Na]^+$ ,

+43  $[\text{AlO}]^+$  and +59  $[\text{AlO}_2]^+$ . This class constituted 5.4% of the total analysed particles. The polar plot (Figure 3) suggests the steelworks cokemaking section as the major source of this particle class. There also appear to be significant contributions from the sinter and blast furnace plants evident in the polar plot, and elevated concentrations of this particle observed at the north-easterly wind sector are suggestive of long range transport of secondary sulphate (Figure 3). Sulphate has also been linked to cokemaking emissions (Konieczynski et al., 2012; Pancras et al., 2013).

### 3.1.2 Silicate dust particle

The **Na- $\text{HSiO}_2$**  particle class occupies 5.2% of the total particles. It is characterized by intense signals at  $m/z$  +23  $[\text{Na}]^+$  in the positive spectrum and  $m/z$  -61  $[\text{HSiO}_2]^-$  in the negative spectrum (Figure 2). Evidence of internal mixing of this particle with EC was found with smaller peaks occurring at  $m/z$  -36, -48, -72 and -144. Nitrate peaks ( $m/z$  -46  $[\text{NO}_3]^-$  and -142  $[\text{NH}_4(\text{NO}_3)_2]^-$ ), and peaks at  $m/z$  -16  $[\text{O}]^-$ , -79  $[\text{PO}_3]^-$ , and -97  $[\text{HSO}_4]^-$  were also identified in this spectrum. Multiple emissions of this particle class from sources such as the blast furnace plant, mills and crustal matter are suggested by the polar plot (Figure 3). Silica is a raw material used in a relatively small proportion (0.3-0.9%) in a blast furnace during steel production (Ricketts, 2013). Silicate particles could originate from erosion and abrasion of local geological materials as well as construction activities (Moreno et al., 2004). The previous work at Port Talbot by Moreno et al. (2004) using scanning electron microscopy revealed silicate particles to constitute 2 and 12% of the total mass of  $\text{PM}_{2.5}$  and  $\text{PM}_{2.5-10}$ , respectively.

The polar plot of the Na- $\text{HSiO}_2$  particle (Figure 3) shows that the presence of this type of particle is associated with higher windspeeds than the Na- $\text{NO}_3$  particle type. The main particle size is intermediate between that of aged sea salt ( $>1 \mu\text{m}$ ) and the combustion-generated particles suggesting that marine aerosol as well as the resuspension of crustal material may be a contributory source.

### 3.1.3 *Ca-rich particle type*

The calcium-rich particle class constituted 2.8% of the total analysed particles. This particle type shows intense spectral peaks at  $m/z$  +40  $[\text{Ca}]^+$ , -46  $[\text{NO}_2]^-$  and -62  $[\text{NO}_3]^-$ . The particle is internally mixed with elemental carbon:  $m/z$  -24  $[\text{C}_2]^-$ , -36  $[\text{C}_3]^-$ , -48  $[\text{C}_4]^-$ , -60  $[\text{C}_5]^-$ , -72  $[\text{C}_6]^-$ , -84  $[\text{C}_7]^-$ , -108  $[\text{C}_9]^-$ , organic carbon:  $-m/z$  -43  $[\text{C}_2\text{H}_3\text{O}]^-$ , phosphate:  $m/z$  -79  $[\text{PO}_3]^-$  and sulphate:  $m/z$  -97  $[\text{HSO}_4]^-$ . A relatively smaller sodium peak  $m/z$  +23  $[\text{Na}]^+$  occurs in this cluster. The polar plot suggests the blast furnace steel production unit as the main contributor to this particle class. Limestone ( $\text{CaCO}_3$ ) and dolomite ( $\text{CaMg}(\text{CO}_3)_2$ ) are key raw materials used in the basic furnace unit of the steel industry (Machemer, 2004).

### 3.1.4 *Carbon-rich particle types*

The carbon-rich particles comprise the following particle classes: Mn-OC, OC, Metallic-EC, OC-EC, EC and EC- $\text{NO}_3$  and account for a total of 24% of analysed particles. The mean aerodynamic diameters of carbon class particles are less than  $1.0 \mu\text{m}$  (Table S1).

The **Mn-OC particle class** is characterized by strong positive peaks at  $m/z$  +39 and +55. A lone strong negative peak was observed at  $m/z$  -26, attributed to  $[\text{CN}]^-$  (Figure 2). Manganese is a notable emission from the steel industry from the ironmaking production unit (Dall'Osto et al., 2008; Mazzei et al., 2008).

However, the spatial pattern of emissions is more consistent with a distributed local low-level source (Figure S1). The spectral peaks at  $m/z$  +39 and +55 could possibly be due to hydrocarbon fragments of  $[\text{C}_3\text{H}_3]^+$  and  $[\text{C}_4\text{H}_7]^+$ , and this seems more plausible than a steel industry source. Published work has reported  $m/z$  +55 as an organic signature co-existing with peaks such as  $m/z$  +27  $[\text{C}_2\text{H}_3]^+$ , +43  $[\text{C}_3\text{H}_7]^+$ , +63  $[\text{C}_5\text{H}_3]^+$  and +77  $[\text{C}_6\text{H}_5]^+$  (Bi et al., 2011; Dall'Osto and Harrison, 2012). Occurrences of  $m/z$  +39  $[\text{K}]^+$  and +55  $[\text{Mn}]^+$  peaks in particles sampled in Shanghai, China

have been attributed to biomass burning (Tao et al., 2011). The origin of this particle type, which has a mean diameter similar to the other carbonaceous particle types (Table S1), remains obscure.

The **Metallic-EC particle** class shows positive spectral signals at  $m/z$  +23 [Na]<sup>+</sup>, +27 [Al]<sup>+</sup>, +48 [Ti]<sup>+</sup>, +56 [Fe]<sup>+</sup>, +59 [AlO<sub>2</sub>], +72 [FeO]<sup>+</sup> and +84 [ZnO]<sup>+</sup>. An elevated peak observed at  $m/z$  +41 might be related to organic carbon [C<sub>3</sub>H<sub>5</sub>]<sup>+</sup>. The negative spectrum is characterized mainly by elemental carbon [C<sub>n</sub>]<sup>-</sup> where  $n=2-9$ . This particle-type may be related to emissions from the hot and cold mills as indicated by the polar plot (Figure 3).

The **EC particle** class shows notable peaks at  $m/z$  [C<sub>n</sub>]<sup>±</sup> ( $n = \pm 2-10$ ). Other peaks occur at [C<sub>n</sub>]<sup>+</sup> ( $n=11$  and  $12$ ) and  $m/z$  +23 [Na]<sup>+</sup>. Among the carbonaceous species, the EC particle class is the most abundant. This particle has a chemical signature (Figure 2) and a polar plot (Figure S1) highly consistent with a source in local traffic emissions.

The **EC-OC particle** class exhibits notable characteristic peaks at  $m/z$  ±36 [C<sub>3</sub>]<sup>±</sup>, +48 [C<sub>4</sub>]<sup>+</sup>, ±60 [C<sub>5</sub>]<sup>±</sup>, -47 [C<sub>3</sub>H<sub>11</sub>]<sup>-</sup>, -72 [C<sub>6</sub>]<sup>-</sup>, -94 [C<sub>7</sub>H<sub>10</sub>]<sup>-</sup> and -97 [HSO<sub>4</sub>]<sup>-</sup>. The presence of  $m/z$  -47 and -94 could also suggest signatures of carbon-containing-halogen particles which are [CCl]<sup>-</sup> and [(CCl)<sub>2</sub>]<sup>-</sup>. See further discussion in the Supplementary Information (Table S2)

The **EC-NO<sub>3</sub> particle** class is another particle observed within the carbonaceous species. The peaks of this particle type occur at  $m/z$  ±36 [C<sub>3</sub>]<sup>±</sup>, ±48 [C<sub>4</sub>]<sup>±</sup>, ±60 [C<sub>5</sub>]<sup>±</sup>, -24 [C<sub>2</sub>]<sup>-</sup>, -46 [NO<sub>2</sub>]<sup>-</sup>, -62 [NO<sub>3</sub>]<sup>-</sup>, -72 [C<sub>6</sub>]<sup>-</sup> and -97 [HSO<sub>4</sub>]<sup>-</sup>. This particle type is moderately correlated with the EC class with correlation ( $r^2$ ) of 0.45. The polar plot (Figure S1) indicates traffic as the probable source with a possible influence from NO<sub>x</sub> emissions from the ironmaking section of the steelworks.



### 3.1.5. Aromatic hydrocarbon (Arom) and PAH particle types

Three particle classes are found within Arom and PAH particle types (Aromatic-PAH-CN, Fe-PAH-NO<sub>3</sub> and PAH-CN) which constitute 12.3% of analysed particles.

The **Aromatic-CN particle** class is characterised by significant spectral signals at  $m/z$  +39 [C<sub>3</sub>H<sub>3</sub>]<sup>+</sup>, +51 [C<sub>4</sub>H<sub>3</sub>]<sup>+</sup>, +63 [C<sub>5</sub>H<sub>3</sub>]<sup>+</sup>, +74 [C<sub>4</sub>H<sub>12</sub>N]<sup>+</sup>, +87 [C<sub>5</sub>H<sub>13</sub>N]<sup>+</sup>, -26 [CN]<sup>-</sup>, -35 [Cl]<sup>-</sup>, -42 [CNO]<sup>-</sup>, -46 [NO<sub>2</sub>]<sup>-</sup>, -49 [C<sub>4</sub>H]<sup>-</sup>, -62 [NO<sub>3</sub>]<sup>-</sup>, -73 [C<sub>6</sub>H]<sup>-</sup> and -97 [HSO<sub>4</sub>]<sup>-</sup>. This particle class shows peaks characteristic of an amide functional group at  $m/z$  +74, +87, -26 and -42. The occurrence of  $m/z$  -49 and -73 in this particle class also indicates fragmentation of PAH and unsaturated organic carbon (Silva and Prather, 2000; Dall'Osto and Harrison, 2012). Traces of PAH could be seen in this cluster at  $m/z$  > 100. The  $m/z$  +39, +51 and +63 might also suggest the presence of [K]<sup>+</sup>, [V]<sup>+</sup> and [Cu]<sup>+</sup>. The polar plot of this particle (Figure 3) shows a clear steelworks emission from the blast furnace (BF) plant (190-270°) and possible contributions from the cokemaking and basic oxygen furnace steelmaking (BOS) sections (170-190°, Table 1). The presence of V might be indicative of a contribution from shipping in the docks area.

The **Fe-PAH-NO<sub>3</sub> particle** class: Elevated peaks of  $m/z$  +23, +43, +56, +63, +189, +202, +215 and +226 are found in the positive spectrum of this cluster while the negative spectrum has peaks at  $m/z$  -35, -46, -62, -79 and -97. This particle class shows low intensity signals for PAH ( $m/z$  > 100) but strong peaks for Fe ( $m/z$  +56), nitrate ( $m/z$  -46 and -62) and sulphate ( $m/z$  -97). The previous study at Port Talbot reported strong  $m/z$  peaks for Fe and PO<sub>3</sub> (FeP particle), which was attributed to emissions from the rolling mill section (Dall'Osto et al., 2008). In the Fe-PAH-NO<sub>3</sub> particle class, there is also evidence of internal mixing of Fe with PO<sub>3</sub> ( $m/z$  -79); though the phosphate peak is weak. A relatively weak peak at  $m/z$  +207 appearing in this particle cluster is suggestive of Pb which has been reported by Dall'Osto et al. (2008). The directional dependence of this particle type (Figure 3) is similar to that of the Arom-CN particle from the steelworks. Temporal correlation is



also quite strong between the Fe-PAH-NO<sub>3</sub> and Arom-CN ( $r^2 = 0.64$ ) particle classes. PAH emissions have been associated with steelworks emissions in many published studies (Tsai et al., 2007; Baraniecka et al., 2010; Brown et al., 2013; Jang et al., 2013). Fe is also a notable emission from the blast furnace (Oravisjarvi et al., 2003; Machemer, 2004; Moreno et al., 2004). Characterisation of particles sampled downwind of an industrial area using a combination of single particle techniques has revealed a particle type composed of an internal mixture of iron oxides and marine-derived particles coated with an organic layer (Sobanska et al., 2014).

**The PAH-CN particle class:** This particle class has a resemblance to both the Arom-CN and Fe-PAH classes (temporal correlation coefficients,  $r^2$  of 0.57 and 0.87, respectively) but with a strong m/z signal at +202, +226, +252, -26, -46 and -97. Peaks are also clearly observed at m/z +43, +63, +189, +215, +276, -35, -49, -62 and -73. This particle is a typical PAH cluster internally mixed with inorganic constituents.

The PAH species represented by m/z +202, 226 and 252 are most likely to be pyrene (mass=202), chrysene (226), benzo[a]pyrene (252), benzo[k]fluoranthene (252) and benzo[b]fluoranthene (252). Some of these PAH constituents have also been reported to be associated with emissions from diesel engines, wood and coal combustion (Lakhani, 2012). The polar plot of the PAH-CN particle class shows an association with steelworks (BF and BOS) emissions and no evidence of a traffic contribution. These similarities among the Arom-CN, Fe-PAH-NO<sub>3</sub> and PAH-CN classes suggest common emission sources with probable origins from the blast furnace, sinter, BOS and cokemaking sections of the steelworks.

### 3.1.6 Aged sea salt particles

The Na-NO<sub>3</sub> particle class represents 5.3% of the total hit particles. It has a mean aerodynamic diameter greater than 1.0  $\mu\text{m}$  (Table S1) and is dominated by sodium (m/z +23) in the positive

spectrum and nitrates in the negative spectrum ( $m/z$  -46 and -62). Smaller peaks are also found at  $m/z$  +39  $[K]^+$ , +62  $[Na_2O]^+$ , +81  $[Na_2Cl]^+$ , -16  $[O]^-$ , -35  $[Cl]^-$ , -93  $[NaCl_2]^-$ , -120  $[NaClNO_3]^-$  and -147  $[Na(NO_3)_2]^-$ . See detailed discussion in the Supplementary Information (Table S2).

### 3.1.7 *Al-Nitrate (AlO-NO<sub>3</sub>) particle type*

Abundance of nitrate spectral peaks at  $m/z$  -46  $[NO_2]^-$  and -62  $[NO_3]^-$  as well as  $m/z$  +43  $[AlO]^+$  are features of this particle class (Figure 2). Smaller peaks are also observed at  $m/z$  -97  $[HSO_4]^-$  and  $m/z$  +137  $[Ba]^+$ . This particle accounted for 4.9% of the total analysed particles. The evidence for a mixed source of secondary nitrate and crustal matter is peculiar to this particle type. Some published work has interpreted  $m/z$  +43 as oxidized organic matter  $[C_2H_3O]^-$  or nitrogen-containing organics  $[CHNO]^+$  (Dall'Osto et al., 2007; Dall'Osto and Harrison, 2012; Smyth et al., 2013) but the unique  $m/z$  +137  $[Ba]^+$  occurring in this cluster could also suggest a crustal or traffic source. Further discussion can be found in the Supplementary Information (Table S2)

## 3.2 Comparison with Previous Studies at Port Talbot

A summary of particle types observed in this present study and that of previous studies is shown in Table S3. Comparing this study with the previous studies involving ATOFMS in Port Talbot (Smith, 2007; Dall'Osto et al., 2008; 2012), newly observed particle types in this study were: K-EC, Mn-OC, metallic-OC, and AlO-Nitrate. The FeP particle type reported by Dall'Osto et al. (2008) has many mass spectral peaks in common with the Fe-PAH-NO<sub>3</sub> particle type observed in this study. However, the Pb, Zn, Fe-rich and Ni particle types reported by Dall'Osto et al. (2008) have no direct analogues. This is surprising especially for the Zn particle type, as elemental analysis revealed significant emissions of this element. Substantial improvements to the emission abatement processes on the steelworks have been implemented over the period since the work of Dall'Osto et al. (2008) and may account for some of the differences. The  $m/z$  signals occurring at  $m/z$  +43  $[AlO]^+$  and 59  $[AlO_2]^+$  are also new (from different particle classes) in this present study compared to

Dall'Osto et al. (2008; 2012). However, an Al particle was reported in the Smith (2007) study. Commonly observed particle types in all these studies are sulphate, aromatic and PAH particles. The evidence of internal mixing of Fe and Mn was not found in this study as also observed in the previous studies possibly due to the instrument low detection efficiency for Mn (Dall'Osto et al., 2008).

### 3.3 Temporal Variations and Polar Plot of Total Particle Number Concentration

Figure S2 shows the temporal variation of total particle number concentration over the four week campaign. Periods with elevated particle counts (greater than 2000 per hour), highlighted with the red circles, were observed on April 19-20, 23-24, 25-26, May 1-2, 6-7 and 9-10. The time series plot of the particle number concentrations for individual particle type is shown in Figure S3. Episodes driven by K-rich particle types appear throughout the sampling period. Four notable peaks were observed for carbonaceous particles on April 19 and 24, and May 2 and 4. Distinctive episodes were also observed for Arom-PAH particle classes. Peaks in the sea salt and silicate dust classes appeared together during some, but not all periods. These results indicate the episodic nature of particle pollution in Port Talbot, and the polar plot of the total ATOFMS particle counts shown in Figure S4 highlights the multiple emission sources of particles. Elevated concentrations observed in the northerly wind sector suggest traffic and residential emissions. At the centre, a high contribution to total particles indicates local traffic emissions. The high particle count in the SE sector suggests steelworks emissions from the hot and cold mills, while elevated particle concentrations from the SW wind sector signify emissions from the steelworks ironmaking section as well as fresh marine aerosol.

### 3.4 Source Contributions by ATOFMS Particles

A summary of particle classes identified by ATOFMS is presented in Table 2. The table also includes the most probable particle sources.

From Table 2, the sources of the ATOFMS particle classes can be broadly categorised into steelworks, traffic, marine, crustal and secondary aerosols. Source contributions of these particle clusters were calculated from their scaled mass concentrations calculated as:  $\text{Mass} = \text{density} \times \text{volume}$ , assuming spherical particle geometry. Scaling was carried out as described by Dall'Osto et al. (2006) and outlined in the experimental section of this paper. Detailed procedures of mass reconstruction of single particles outlined in Dall'Osto et al. (2006), were not applied to individual chemical elements. Results for the source contributions to the sampled particles are shown in Figure 4. The combined steelworks (BF/Sinter+/Mills/Cokemaking+Mills) shows the highest contribution (45%) to the total (ATOFMS) particles followed by traffic (28%) and marine sources (14%). The Al-Nitrate( $\text{Al-NO}_3$ ) account for a total contribution of 4%. As depicted in their polar plots (see Figure S1) nitrate particles were related with traffic emissions. Crustal matter contributed 9% to the total single particles during the sampling. Such results are inevitably subject to much uncertainty as many of the particle types reflect mixed sources contributing to a single particle, or multiple sources of a particle type.

### 3.5 Comparison of ATOFMS with Receptor Models

ME-2 receptor modelling of filter-based measurement data (Partisol and Streaker) has been reported elsewhere (Crawford et al., 2005; Amato et al. 2010; Amato and Hopke, 2012), and this method has been applied to data from the Port Talbot steelworks (Taiwo et al, 2014b).

The ME-2 source apportionment study was based upon hourly data derived from samples collected on a Streaker sampler and daily samples collected with a Partisol instrument co-located with the ATOFMS at the Fire Station site. The mass concentration of  $\text{PM}_{2.5}$  derived from the Partisol filters was  $7.4 \mu\text{g m}^{-3}$  averaged over the entire campaign. In comparison, the sum of particle masses derived from the ATOFMS data amounted to  $9.8 \mu\text{g m}^{-3}$  indicating a reasonable agreement but some over-estimation in the ATOFMS data. Since the largest particles measured by the ATOFMS

were 1.9  $\mu\text{m}$  aerodynamic diameter and the Partisol size cut was at 2.5  $\mu\text{m}$ , it would be expected that the Partisol measurements would be somewhat higher than those estimated from the ATOFMS although the proportion of  $\text{PM}_{10}$  mass in the 1.9-2.5  $\mu\text{m}$  diameter range was relatively small (Taiwo et al., 2014a). The over-estimation from the ATOFMS data most probably therefore relates to the choice of density for the various particle types, perhaps allowing inadequately for the internal mixing of the metallic particles.

It is not straightforward to compare the ATOFMS mass assignments to those derived from the ME-2 source apportionment since the particle classes are different. Particle classes which might be expected to be comparable between the ATOFMS and ME-2 data are the traffic and marine particle classes. The ME-2 analysis attributed 13% of  $\text{PM}_{2.5}$  mass to the traffic source whereas the attribution from the ATOFMS data is 28%. A slightly better agreement is seen for marine aerosol with 20% from ME-2 and 14% for the ATOFMS. A large difference is seen in relation to emissions from the steelworks, although a definitive comparison is not possible as the ME-2 results attribute 27% of  $\text{PM}_{2.5}$  mass to a mixed ammonium sulphate and steelworks factor. ME-2 also attributes 14% of  $\text{PM}_{2.5}$  mass to other steelworks sources while the ATOFMS attributes in total 45% of measured mass to the steelworks sources. Consequently, even if the ammonium sulphate/steelworks factor from the ME-2 were to be assumed wholly from the steelworks, it would still give a lower estimate of the mass contribution from the steelworks than from the ATOFMS data. The largest difference relates to the secondary component. The ME-2 analysis attributes 20% of  $\text{PM}_{2.5}$  mass to ammonium nitrate and 27% to the mixed ammonium sulphate/steelworks factor giving a potential total of 47%. However, the ATOFMS results show the presence of sulphate and nitrate in many of the particle classes including particularly those attributed to road traffic and to emissions from the steelworks. Consequently, the attribution of mass to secondary particles based upon the ATOFMS data is very small (4%) and clearly a very substantial under-estimate of the

secondary particle contribution which is known to be substantial at this site (see e.g. Taiwo et al., 2014a).

The ATOFMS instrument has assisted in identifying important steelworks marker elements which have been used for source apportionment by filter-based measurement. Fe, Mn and Ca are important steelworks emissions from the BF plant (Machemer, 2004; Mazzei et al., 2008; Hleis et al., 2013). Ca-rich particles were identified by the ATOFMS instrument with the polar plot revealing the blast furnace unit as the source. A Ca-rich particle type represented approximately 3% of the total analysed ATOFMS particles (Table 2), and was comparable with the blast furnace factor of the Streaker ME-2 for PM<sub>2.5</sub>. Ca is the third most abundant element (18% of ME-2 modelled concentration) apportioned to the blast furnace factor after Fe (52%) and Mn (51%). The scaled ATOFMS mass size distribution of Ca shows two peaks in the fine and coarse modes indicative of emissions from the steelworks and crustal sources respectively. However, the elevated fine peak of Ca demonstrates dominance of steelworks emissions (from the blast furnace). This trend was observed for silica particles but with a relatively small peak in the fine mode probably due to the relatively small use in steel production (Ricketts, 2013). The Fe-PAH-NO<sub>3</sub> particle type was also identified by the ATOFMS and indicated BF/Sinter emissions. Fe and Mn might not have occurred in the same particle type with Ca but not be detected due to low detection efficiency of the instrument for these metals compared to Ca (Dall'Osto et al., 2008). It should be however, noted that the ATOFMS instrument was able to identify Mn and Fe spectral signals in other particle types (e.g. Mn-OC and Fe-PAH particles).

The carbon and aromatic/polycyclic aromatic hydrocarbon particle groups accounted for 24% of the number of classified particles (Table 2). Most of the carbon type particles were associated with local traffic emissions. The aromatic/PAH particle groups revealed the cokemaking and BOS sections of the steelworks as the major emitters. These organic constituents were not included in the

analysis of Partisol filters and hence do not allow direct comparison with ATOFMS apportioned particles. However, the evidence for steelworks emission of organics such as aromatic and polycyclic aromatic hydrocarbon from the ATOFMS instrument is strong. A number of studies based on filter and single particle measurements have previously reported elevated concentrations of organics around steelworks sites (Yang et al., 2002; Manoli et al., 2004; Liberti et al., 2006; Choi et al., 2007; Tsai et al., 2007; Dall'Osto et al., 2012).

#### 4. CONCLUSIONS

Single particle analysis using the ATOFMS is useful for source identification and apportionment of particulate matter. With the assistance of ENCHILADA software, 20 clusters, which were subsequently grouped into 17 clusters, were identified. These clusters were classified into 8 particle groups viz: K-rich, sea salt, silica dust, sulphate, nitrate, Ca-rich, carbonaceous and Arom/PAH, which accounted for 96% of successfully ionized particles. Among the species identified by ATOFMS, K-rich particles represented the highest percent (52%), followed by carbon-rich particles (24%). Arom/PAH, aged sea salt, silica dust, sulphate, nitrate and Ca particles constituted 12, 5, 5, 5, 5 and 3%, respectively. This apportionment is, however, likely to be influenced by the extremely high sensitivity of the ATOFMS to potassium, which has not been controlled for. The polar plots of individual clusters indicate that fine PM in Port Talbot is mainly from marine, steelworks, traffic and mineral dust sources. The steelworks showed the greatest contribution to ATOFMS particles representing 45% of the apportioned particles. Out of the 17 particle clusters, 11 exhibited a signature associated with the steelworks; these include: K-CN, K-EC, K-Cl-PO<sub>3</sub>, K-HSO<sub>4</sub>, Ca, Mn-OC, Metallic-EC, Arom-CN, Fe-PAH-NO<sub>3</sub> and PAH-CN. The unscaled ATOFMS particle number concentration showed temporal variations largely driven by K-rich particles. The single particle analysis using ATOFMS has provided further information on the contribution of the steelworks to PM pollution in Port Talbot with BF/Sinter plants representing the major emission sources. Emissions from the steelworks cold and hot mills section, which had not been identified with the



ME-2 receptor model, were clearly revealed by ATOFMS. The rapid response of the ATOFMS allowing particles to be associated with specific wind directions is a major benefit compared to bulk analytical methods.

The comparison of the source apportionment of particle mass from the ATOFMS data with that derived from application of the ME-2 receptor model to simultaneously collected chemically speciated PM<sub>2.5</sub> data reveals important differences. Most importantly, the extensive internal mixing of sulphate and nitrate with other constituents in particles detected by the ATOFMS makes it very difficult to identify clearly a contribution of secondary particles to the ATOFMS mass data. Both constituents are regularly measured but the nitrate is frequently associated with carbonaceous particles with an evident traffic source. Sulphate appears in many particle types including a number which originate from the steelworks and it is unclear to what extent the mass should be attributed to the local steelworks source or to regional transport of sulphate aerosol. As a consequence the ATOFMS attributes a greater percentage of measured mass to the traffic source than the ME-2 receptor model while ME-2 identifies a substantial ammonium nitrate contribution to mass which far exceeds the secondary nitrate contribution suggested by the ATOFMS data. The attribution of mass to marine aerosol is broadly similar between the two methods. It would appear that the main strength of the ATOFMS when combined with wind sector analysis is in identifying particle types originating from the steelworks. However, due to substantial internal mixing of particles, quantitative attribution of particle mass at the measurement site to steelworks emissions remains extremely difficult. Judging from the comparison with the ME-2 receptor model data, the ATOFMS attribution of particle mass to the steelworks is probably substantially over-estimated.

## ACKNOWLEDGEMENT

We are grateful for support from the National Centre for Atmospheric Science (NCAS) which is funded by the UK Natural Environment Research Council and for support to Adewale Taiwo from



the Tertiary Education Trust Fund (TETFund), Federal University of Agriculture, Nigeria and for support to Zongbo Shi from Natural Environment Research Council. Furthermore, we would like to formally thank Neath-Port Talbot Council, the Environment Agency Wales, Mid and West Wales Fire and Rescue Service, Dwr Cymru and Dyffryn School, Port Talbot for hosting our measurements.

## REFERENCES

- Amato, F., Pandolfi, M., Querol, X., Alastuey, A., Pey, J., Luís J.J., 2010. Application of receptor modelling techniques (PMF2, ME-2, PCA) to rural and urban PM measurements performed during DAURE Campaign. EGU General Assembly 2010, held 2-7 May, 2010 in Vienna, Austria, p.11587.
- Amato, F., Hopke, P.K., 2012. Source apportionment of the ambient PM<sub>2.5</sub> across St. Louis using constrained positive matrix factorization, *Atmos. Environ.*, 46, 329-337.
- AQEG, 2011. Understanding PM<sub>10</sub> in Port Talbot. Advice note prepared for Department of Environment, Food and Rural Affairs: Scottish, Welsh Assembly Government, and Department of the Environment, Northern Ireland. [uk-air.defra.gov.uk/...110322\\_AQEG\\_Port\\_Talbot\\_Advice\\_Note.pdf](http://air.defra.gov.uk/...110322_AQEG_Port_Talbot_Advice_Note.pdf). Accessed on 04/01/13.
- Ault, A.P., Gaston, C.J., Wang, Y., Dominguez, G., Thiemens, M.H., Prather, K.A., 2010. Characterization of the single particle mixing state of individual ship plume events measured at the Port of Los Angeles. *Environ. Sci. Technol.*, 44(6), 1954-1961, doi:10.1021/es902985h.
- Baraniecka, J., Pyrzynska, K., Szewczynska, M., Posniak, M., Dobrzynska, E., 2010. Emission of polycyclic aromatic hydrocarbons from selected processes in steelworks. *Journal of Hazardous Materials* 183, 111-115.
- Bein, K.J., Zhao, Y., Johnston, M.V., Wexler, A.S., 2007. Identification of sources of atmospheric PM at the Pittsburgh Supersite--Part III: Source characterization. *Atmos. Environ.*, 41(19), 3974-3992.
- Bein, K.J., Zhao, Y., Pekney, N.J., Davidson, C.I., Johnston, M.V., Wexler, A.S., 2006. Identification of sources of atmospheric PM at the Pittsburgh Supersite--Part II: Quantitative comparisons of single particle, particle number, and particle mass measurements. *Atmos. Environ.*, 40(Supplement 2), 424-444.
- Bi, X.H., Zhang, G.H., Li, L., Wang, X.M., Li, M., Sheng, G.Y., Fu, J.M., Zhou, Z., 2011. Mixing state of biomass burning particles by single particle aerosol mass spectrometer in the urban area of PRD, China. *Atmos. Environ.*, 45, 3447-3453.
- Brown, A.S., Brown, R.J., Coleman, P., Conolly, C., Sweetman, A., Jones, K.C., Butterfield, D. M., Sarantaridis, D., Donovan, B.J., Roberts, I., 2013. Twenty years of measurement of polycyclic aromatic hydrocarbons (PAHs) in UK ambient air by nationwide air quality networks. *Environmental Science: Processes Impacts* 15, 1199-1215.
- Chemical Book, 2008. Carbon Black (1333-86-4). [www.chemicalbook.com/ProductMSDS/DetailCB310908\\_EN.htm](http://www.chemicalbook.com/ProductMSDS/DetailCB310908_EN.htm). Accessed: 09/11/13.
- Choi, S.-D., Baek, S.-Y., Chang, Y.-S., 2007. Influence of a large steel complex on the spatial distribution of volatile polycyclic aromatic hydrocarbons (PAHs) determined by passive air sampling using membrane-enclosed copolymer (MECOP). *Atmos Environ.*, 41, 6255-6264.

- Crawford, J.A., Cohen, D.D., Dyer, L.L., Zahorowski, W., 2005. Receptor modelling with PMF2 and ME2 using aerosol data from Hong Kong. Australian Nuclear Science and Technology Organisation Publication. <http://apo.ansto.gov.au/dspace/handle/10238/201>. Accessed: 30/11/13.
- Dall'Osto, M., Drewnick, F., Fisher, R., Harrison, R.M., 2012. Real-time measurements of non-metallic fine particulate matter adjacent to a major integrated steelworks. *Aerosol Sci. Technol.* 46, 639-653.
- Dall'Osto, M., Harrison, R.M., 2012. Urban organic aerosols measured by single particle mass spectrometry in the megacity of London. *Atmos. Chem. Phys.* 12, 4127-4142.
- Dall'Osto, M., Booth, M.J., Smith, W., Fisher, R., Harrison, R.M., 2008. Study of the size distributions and the chemical characterization of airborne particles in the vicinity of a large integrated steelworks. *Aerosol Sci. Technol.* 42, 981-991.
- Dall'Osto, M., Harrison, R.M., Charpantodou, E., Loupa, G., Rapsomanikis, S., 2007. Characterisation of indoor airborne particles by using real-time aerosol mass spectrometry. *Sci Tot Environ.* 384, 120-123.
- Dall'Osto, M., Harrison, R.M., 2006. Chemical characterization of single airborne particles in Athens (Greece) by ATOFMS. *Atmos. Environ.*, 40, 7614-7631.
- Dall'Osto, M., Harrison, R.M., Beddows, D.C.S., Feeney, Heal, M.R., Donovan, R.J., 2006. Single particle detection efficiencies of aerosol time-of-flight mass spectrometry during the North Atlantic marine boundary layer experiment. *Environ. Sci Technol.* 40, 5029 – 5035.
- Dall'Osto, M., Beddows, D.C.S., Kinnersley, R.P., Harrison, R.M., Donovan, R.J., Heal, M.R. (2004). Characterization of individual airborne particles by using aerosol time-of-flight mass spectrometry at Mace Head, Ireland. *J. Geophys. Res. Atmospheres* 109 (D21), D21302.
- Dan, M., Zhuang, G., Li, X., Tao, H., Zhuang, L., 2004. The characteristics of carbonaceous species and their sources in PM<sub>2.5</sub> in Beijing. *Atmos. Environ.* 38, 3443-3452.
- Eatough, D.J., Grover, B.D., Woolwine, W.R., Eatough, N.L., Long, R., Farber, R., 2008. Source apportionment of 1 h semi-continuous data during the 2005 Study of Organic Aerosols in Riverside (SOAR) using positive matrix factorization. *Atmos. Environ.*, 42(11), 2706-2719.
- Gard, E.E., Mayer, J.E., Morrical, B.D., David, T.D., Fergenson, P., Prather, K.A., 1997. Real-Time Analysis of Individual Atmospheric Aerosol Particles: Design and Performance of a Portable ATOFMS. *Anal. Chem.* 69, 4083-4091.
- Gietl, J.K., Lawrence, R., Thorpe, A.J., Harrison, R.M., 2010. Identification of brake wear particles and derivation of a quantitative tracer for brake dust at a major road. *Atmos. Environ.* 44, 141-146.
- Giorio, C., Tapparo, A., Dall'Osto, M., Harrison, R. M., Beddows, D.C.S., DiMarco, C., Nemitz, E., 2012. Comparison of three techniques for analysis of data from an Aerosol Time-of-Flight Mass Spectrometer. *Atmos. Environ.* 61, 316-326.
- Gross, D.S., Galli, M.E., Silva, P.J., Prather, K.A., 2000. Relative sensitivity factors for alkali metal and ammonium cations in single particle aerosol time-of-flight mass spectra. *Analytical Chemistry* 72 (2):416-22.

- Gysel, M., Crosier, J., Topping, D.O., Whitehead, J.D., Bower, K.N., Cubison, M.J., Williams, P., Flynn, M., McFiggans, G., Coe, H., 2007. Closure between chemical composition and hygroscopic growth of aerosol particles during TORCH2, in nucleation and atmospheric aerosols, edited by C. O'Dowd and P. Wagner, pp. 731-735, Springer Netherlands, doi:10.1007/978-1-4020-6475-3\_144.
- Harrison, R. M., Beddows, D. C. S., Hu, L., Yin, J. (2012a). Comparison of methods for evaluation of wood smoke and estimation of UK ambient concentrations. *Atmos. Chem. Phys.* 12, 8271-8283.
- Harrison, R.M., Jones, A., Gietl, J., Yin, J., Green D., 2012b. Estimation of the contribution of brake dust, tire wear and resuspension to nonexhaust traffic particles derived from atmospheric measurements. *Environ.Sci Technol.* 46, 6523-6529.
- Healy, R.M., Sciare, J., Poulain, L., Crippa, M., Wiedensohler, A., Prevot, A.S.H., Baltensperger, U., Sarda-Esteve, R., McGuire, M.L., Jeong, C.-H., McGillicuddy, E., O'Connor, I.P., Sodeau, J. R., Evans, G.J., Wenger, J.C., 2013. Quantitative determination of carbonaceous particle mixing state in Paris using single particle mass spectrometer and aerosol mass spectrometer measurements. *Atmos. Chem. Phys.* 13, 9479-9496.
- Healy, R.M., Hellebust, S., Kourtchev, I., Allanic, A., O'Connor, I.P., Bell, J.M., Healy, D.A., Sodeau, J.R., Wenger, J.C., 2010. Source apportionment of PM<sub>2.5</sub> in Cork Harbour, Ireland using a combination of single particle mass spectrometry and quantitative semi-continuous measurements. *Atmos. Chem. Phys.*, 10(19), 9593-9613, doi:10.5194/acp-10-9593-2010.
- Healy, R.M., O'Connor, I.P., Hellebust, S., Allanic, A., Sodeau, J.R., Wenger, J.C., 2009. Characterisation of single particles from in-port ship emissions. *Atmos. Environ.*, 43(40), 6408-6414.
- Held, A., Hinz, K-P., Trimborn, A., Spengler, B., Klemm, O., 2002. Chemical classes of atmospheric aerosol particles at a rural site in Central Europe during Winter. *J. Aerosol Sci.* 33, 581-594.
- Hleis, D., Fernandez-Olmo, I., Ledoux, F., Kfoury, K., Courcot, L., Desmonts, T., Courcot, D., 2013. Chemical profile identification of fugitive and confined particle emissions from an integrated iron and steelmaking plant. *J. Hazard.Mater.* 250-251, 246-255.
- Jang, E., Alam, M. S., Harrison, R.M., 2013. Source apportionment of polycyclic aromatic hydrocarbons in urban air using Positive Matrix Factorization and spatial distribution analysis. *Atmos. Environ.* 79, 271-285.
- Kelly, K.E., Sarofim, A.F., Lighty, J.S., Arnott, W.P., Rogers, C.F., Zielinska, B., Prather, K.A., 2003. User guide for characterizing particulate matter: Evaluation of several real-time methods. <http://ds.heavyoil.utah.edu/dspace/handle/123456789/10315>. Accessed 15/07/13.
- Konieczynski, J., Zajusz-Zubek, E., Jabłonska, M., 2012. The release of trace elements in the process of coal coking. *Scientific World J.* 2012, Article ID 294927, doi:10.1100/2012/294927.
- Lakhani, A., 2012. Source apportionment of particle bound polycyclic aromatic hydrocarbons at an industrial location in Agra, India. *Scientific World J.* 2012, Article ID 781291, doi: 10.1100/2012/781291.

- Li, J., Posfai, M., Hobbs, P.V., Buseck, P.R., 2003. Individual aerosol particles from biomass burning in southern Africa: 2, Compositions and aging of inorganic particles. *J. Geophys. Res.* 108 (D13), 8484. doi:10.1029/2002JD002310.
- Liberti, L., Notarnicola, M., Primerano, R., Zannetti, P., 2006. Air pollution from a large steel factory: polycyclic aromatic hydrocarbon emissions from coke-oven batteries. *JAWMA* 56, 255-260.
- Machemer, S.D., 2004. Characterization of airborne and bulk particulate from iron and steel manufacturing facilities. *Environ. Sci. Technol.* 38, 381-389.
- McGuire, M.L., Jeong, C.H., Slowik, J.G., Chang, R.W., Corbin, J.C., Lu, G., Mihele, C., Rehbein, P.J.G., Sills, D.M.L., Abbatt, J.P.D., Brook, J.R., Evans, G. J., 2011. Elucidating determinants of aerosol composition through particle-type-based receptor modelling. *Atmos. Chem. Phys.*, 11(15), 8133-8155, doi:10.5194/acp-11-8133-2011.
- Mackay, D., Shiu, W.Y., Ma, K.-C., Lee, S.C., 2006. Handbook physical-chemical properties and environmental fate for organic chemical. Taylor and Francis Group, New York. <http://files.rushim.ru/books/spravochniki/mackay1.pdf>. Accessed: 09/11/13.
- Manoli, E., Kouras, A., Samara, C., 2004. Profile analysis of ambient and source emitted particle-bound polycyclic aromatic hydrocarbons from three sites in northern Greece. *Chemosphere* 56, 867-878.
- Mazzei, F., D'Alessandro, A., Lucarelli, Nava, S., Prati, P., Valli, G., Vecchi, R., 2008. Characterization of particulate matter sources in an urban environment. *Sci. Tot. Environ.* 401, 81-89.
- Moffet, R.C., de Foy, B., Molina, L.T., Molina, M.J., Prather, K.A., 2008). Measurement of ambient aerosols in northern Mexico City by single particle mass spectrometry. *Atmos. Chem. Phys.* 8, 4499-4516.
- Moreno, T., Jones, T.P., Richards, R.J., 2004. Characterisation of aerosol particulate matter from urban and industrial environments: examples from Cardiff and Port Talbot, South Wales, UK. *Sci. Tot. Environ.* 334-335, 337-346.
- Oravissjarvi, K., Timonen, K. L., Wiikinkoski, T., Ruuskanen, A. R. Heinanen, K., Ruuskanene, J., 2003. Source contributions to PM<sub>2.5</sub> particles in the urban air of a town situated close to a steel works. *Atmos. Environ.* 37, 1013-1022.
- Owega, S., Khan, B.-U.-Z., D'Souza, R., Evans, G.J., Fila, M., Jervis, R.E. 2004. Receptor modeling of Toronto PM<sub>2.5</sub> characterized by Aerosol Laser Ablation Mass Spectrometry, *Environ. Sci. Technol.*, 38(21), 5712-5720, doi:10.1021/es035177i.
- Pancras, J.P., Landis, M.S., Norris, G.A., Vedantham, R., Dvonch, J.T., 2013. Source apportionment of ambient fine particulate matter in Dearborn, Michigan, using hourly resolved PM chemical composition data. *Sci. Tot. Environ.* 448, 2-13.

- Phillips, S. L., Perry, D.L.(1995). Handbook of Inorganic Compounds, CRC Press, Boca Raton, FL.
- Prather, K.A., 1998. Aerosol Time-of-Flight Mass Spectrometry (ATOFMS) as a Real-Time Monitor of Individual Aerosol Particles in Field Studies. Contract 95-305. <http://www.arb.ca.gov/research/apr/past/95-305.pdf>. Accessed: 29/08/13.
- Prather, K.A., Nordmeyer, T., Salt, K., 1994. Real-time characterization of individual aerosol particles using time-of-flight mass spectrometry. *Anal.Chem.* 66, 1403-1407.
- Reinard, M.S., Adou, K., Martini, J.M., Johnston, M.V., 2007. Source characterization and identification by real-time single particle mass spectrometry. *Atmos. Environ.*, 41(40), 9397-9409.
- Ricketts, J.A., 2013. How a blast furnace works. American Iron and Steel Institutes, <http://www.steel.org/Making%20Steel/How%20Its%20Made/Processes/How%20A%20Blast%20Furnace%20Works%20larry%20says%20to%delete.aspx>. Accessed: 26/06/13.
- Silva, P.J., Prather, K.A., 2000. Interpretation of mass spectra from organic compounds in aerosol time-of-flight mass spectrometry. *Anal. Chem.* 72, 3553-3562.
- Smith, W. 2007. High time resolution chemical fingerprinting and source apportionment of atmospheric particulate emissions from the steel industry. PhD Thesis. School of Geography, Earth and Environmental Sciences. The University of Birmingham, UK. 434p.
- Smyth, A.M., Thompson, S.L., de Foy, B., Olson, M. R., Sager, N., McGinnis, J., Schauer, J.J., Gross, D.S., 2013. Sources of metals and bromine-containing particles in Milwaukee. *Atmos. Environ.* 73, 124-130.
- Sobanska, S., Falgayrac, G., Rimetz-Planchon, J., Perdrix, E., Bremard, C., Barbillat, J., 2014. Resolving the internal structure of individual atmospheric aerosol particle by the combination of atomic force microscopy, ESEM-EDX, Raman and ToF-SIMS imaging. *Microchem. J.* 114, 89-98.
- Sullivan, R.C., Guazzotti, S.A., Sodeman, D.A., Tang, S., Carmichael, G.R., Prather, K.A., 2007. Mineral dust is a sink for chlorine in the marine boundary layer. *Atmos. Environ.* 41, 7166-7179.
- Sullivan, R.C., Prather, K.A., 2005. Recent advances in our understanding of atmospheric chemistry and climate made possible by online aerosol analysis instrumentation. *Anal. Chem.* 77, 3861-3885.
- Snyder, D.C., Schauer, J.J., Gross, D.S., Turner, J.R., 2009. Estimating the contribution of point sources to atmospheric metals using single-particle mass spectrometry. *Atmos. Environ.*, 43(26), 4033-4042.
- Taiwo, A.M., Beddows, D.C.S., Shi, Z. and Harrison, R.M., 2014a. Mass and number size distributions of particulate matter components: Comparison of an industrial site and an urban background site. *Sci. Tot. Environ.*, 475, 29-38.
- Taiwo, A.M., Beddows D.C.S., Calzolari, C., Harrison, R.M., Lucarelli, F., Nava, S., Shi, Z., Valli, G., Vecchi R., 2014b. Receptor modelling of airborne particulate matter in the vicinity of a major steelworks site. *Sci.Tot.EnvIRON.*490, 488-500.
- Tao, S., Wang, X., Chen, H., Yang, X., Li, M., Zhou, Z., 2011. Single particle analysis of ambient aerosols in Shanghai during the World Exposition, 2010: two cases studies. *Frontier Environ. Sci. Engineer. China* 5, 391-401.



819 Tsai, J.-H., Lin, K.-H., Chen, C.-Y., Ding, J.-Y., Choa, C.-G., Chiang, H.-L., 2007. Chemical  
820 constituents in particulate emissions from integrated iron and steel facility. *J. of Hazard.Mater.* 147,  
821 111-119.

822  
823 Yang, H-H., Lai, S.-O., Hsieh, L-T., Hsueh, H-J., Chi, T.-W., 2002. Profiles of PAH emission from  
824 steel and iron industries. *Chemosphere* 48, 1061–1074.

825

**TABLE LEGENDS**

**Table 1:** Wind sectors linking the steelworks processes with the ATOFMS sampling site.

**Table 2:** Summary of the particle cluster emission sources.

**FIGURE LEGENDS**

**Figure 1:** Port Talbot sampling station and the steelworks processing unit.

**Figure 2:** Attribution of particle clusters to source categories

**Figure 3:** Polar plots of steelworks particle clusters

**Figure 4:** Source contribution of particles derived from ATOFMS types.



**Table 1:** Wind sectors linking the steelworks processes with the ATOFMS sampling site

Sector/plant	Fire Station
<b><i>Ironmaking</i></b> Sinter plant Blast furnace Raw materials	190–270°
<b><i>Steelmaking/cokemaking</i></b> BOS plant Cokemaking	170–190°
<b><i>Mills</i></b> Hot mill Cold mill	150–170°

846

847 **Table 2:** Attribution of particle clusters to source categories.

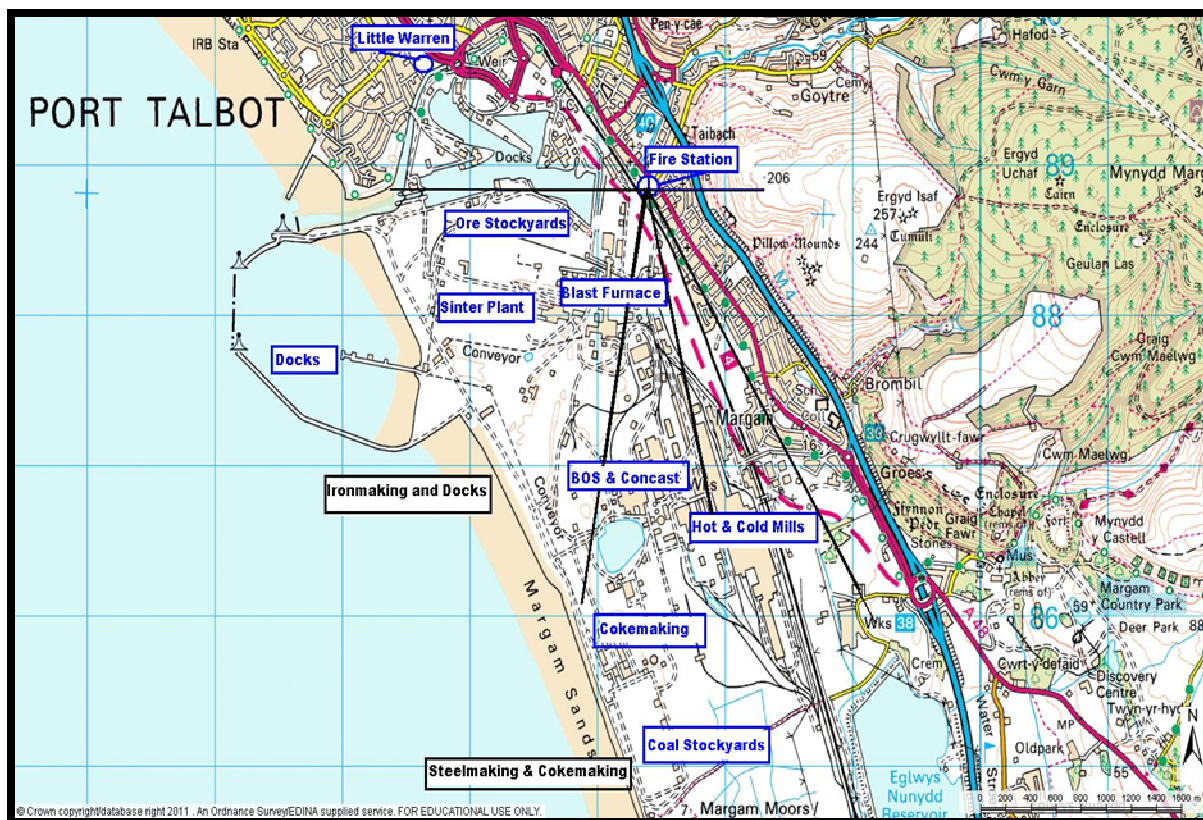
	Particle Classes	Clusters	All Emissions Sources	Strong Emissions Sources	% of Particles
1	K-rich	K-CN	Cokemaking/Mills	Cokemaking/Mills	11.4%
2		K-NO <sub>3</sub>	Traffic/Biomass	Traffic	16.6%
3		K-EC	Cokemaking/Mills/ Biomass	Cokemaking/Mills	7.2%
4		K-Cl-PO <sub>3</sub>	BF/Sinter/Mills	BF/Sinter	11.1%
5	Sea Salt	Na-NO <sub>3</sub>	Marine	Marine	5.3%
6	Silicate Dust	Na-HSiO <sub>2</sub>	Crustal	Crustal	5.2%
7	Sulphate	K-HSO <sub>4</sub>	Cokemaking/Mills/ Secondary	Cokemaking/Mills	5.4%
8	Nitrate	AlO-NO <sub>3</sub>	Traffic/Secondary	Traffic	4.9%
9	Ca-rich	Ca	BF/sinter	BF/sinter	2.8%
10	Carbonaceous	Mn-OC	Cokemaking/Mills	Cokemaking/Mills	0.3%
11		Metallic-EC	Mills	Mills	3.7%
12		EC-OC	Traffic	Traffic	2.6%
13		EC	Traffic	Traffic	9.1%
14		EC-NO <sub>3</sub>	Traffic	Traffic	2.0%
15	Arom-PAH	Aromatic-CN	BF/Sinter/BOS/ Cokemaking	BF/Sinter	4.5%
16		Fe-PAH-NO <sub>3</sub>	BF/Sinter/BOS/ Cokemaking	BF/Sinter	4.5%
17		PAH-CN	BF/Sinter/BOS/ Cokemaking	BF/Sinter	3.3%

848 BF-blast furnace, BOS-basic oxygen furnace steelmaking

849

850

851



852

853

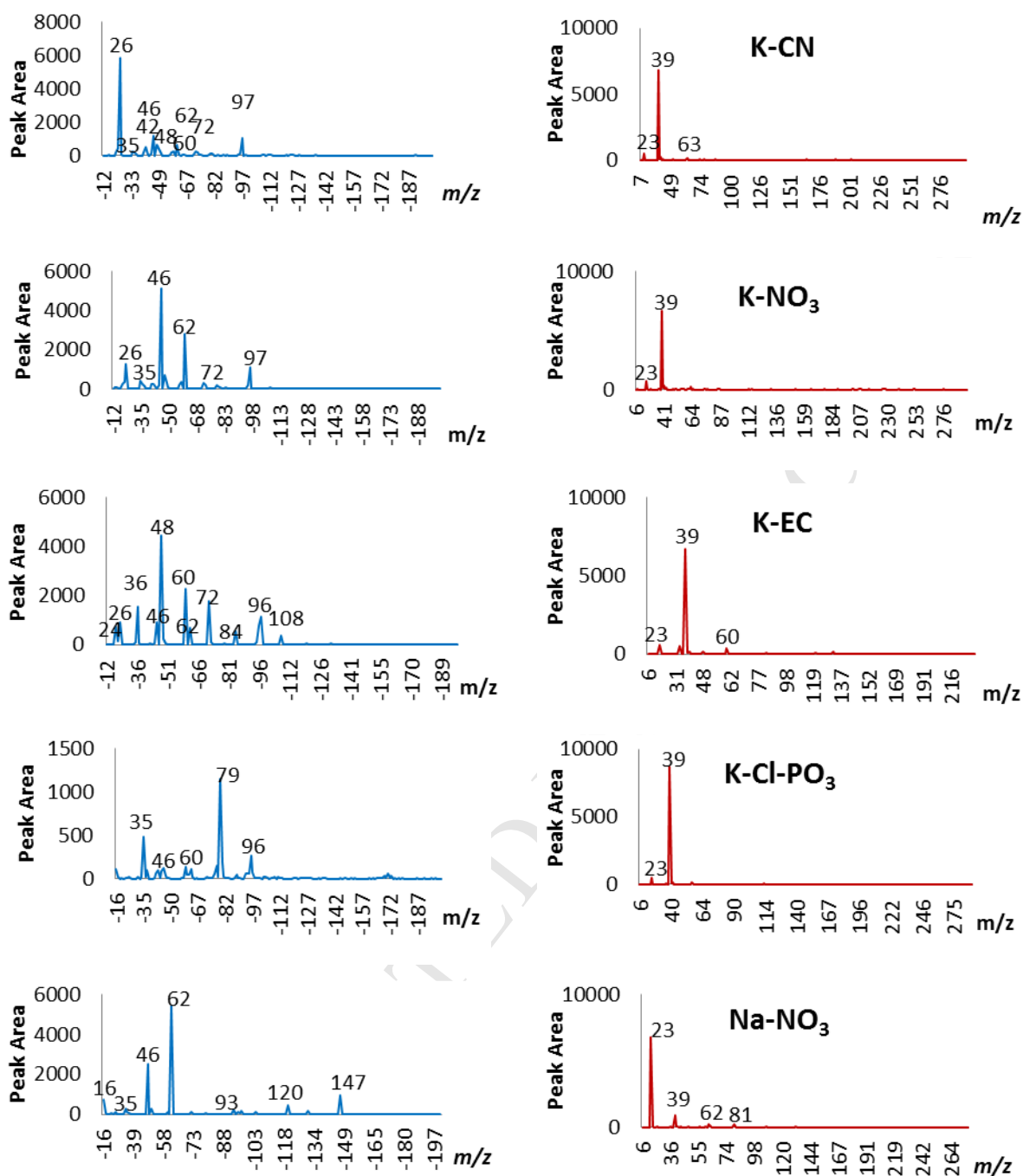
854

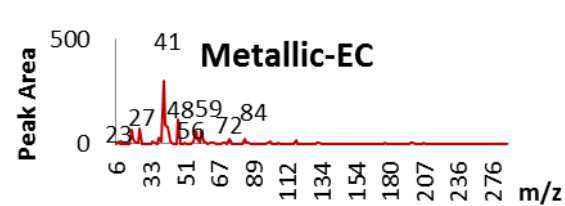
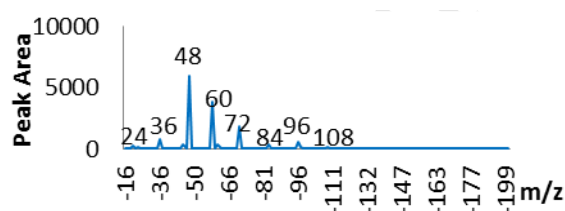
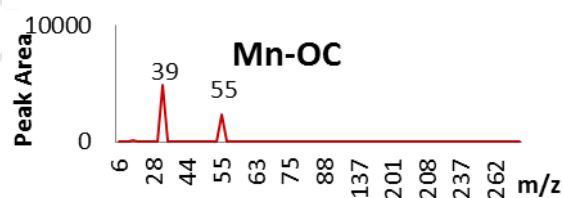
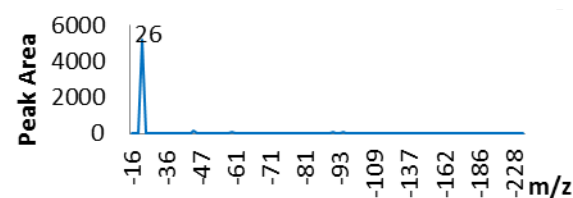
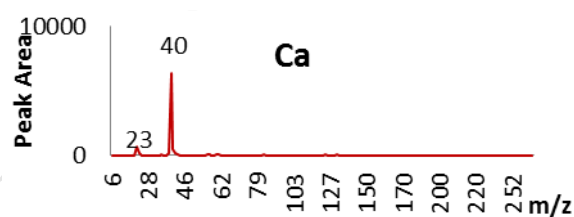
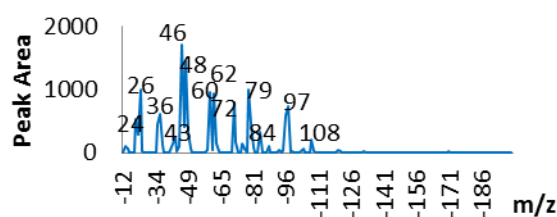
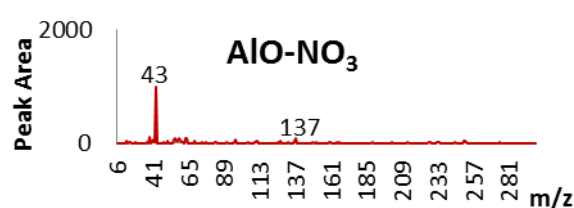
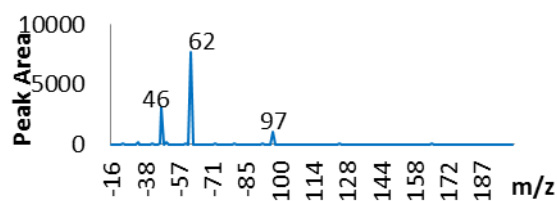
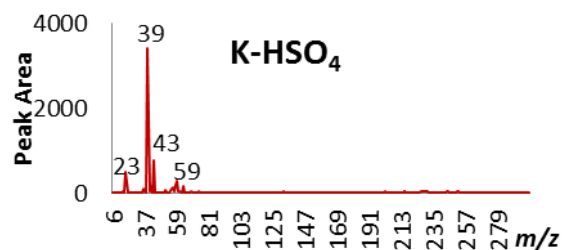
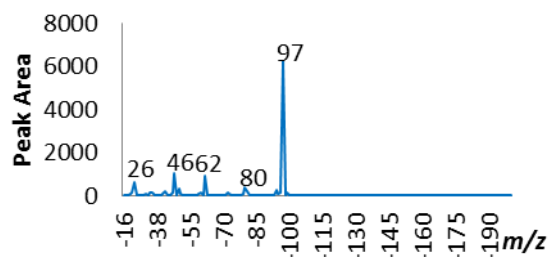
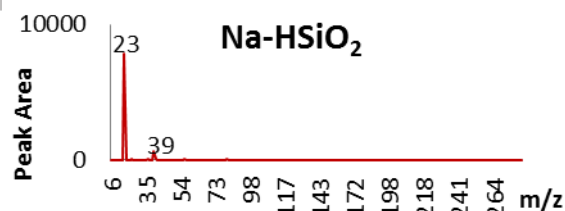
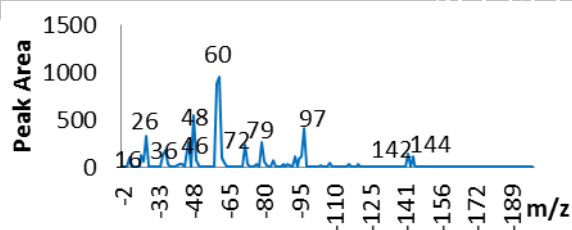
855

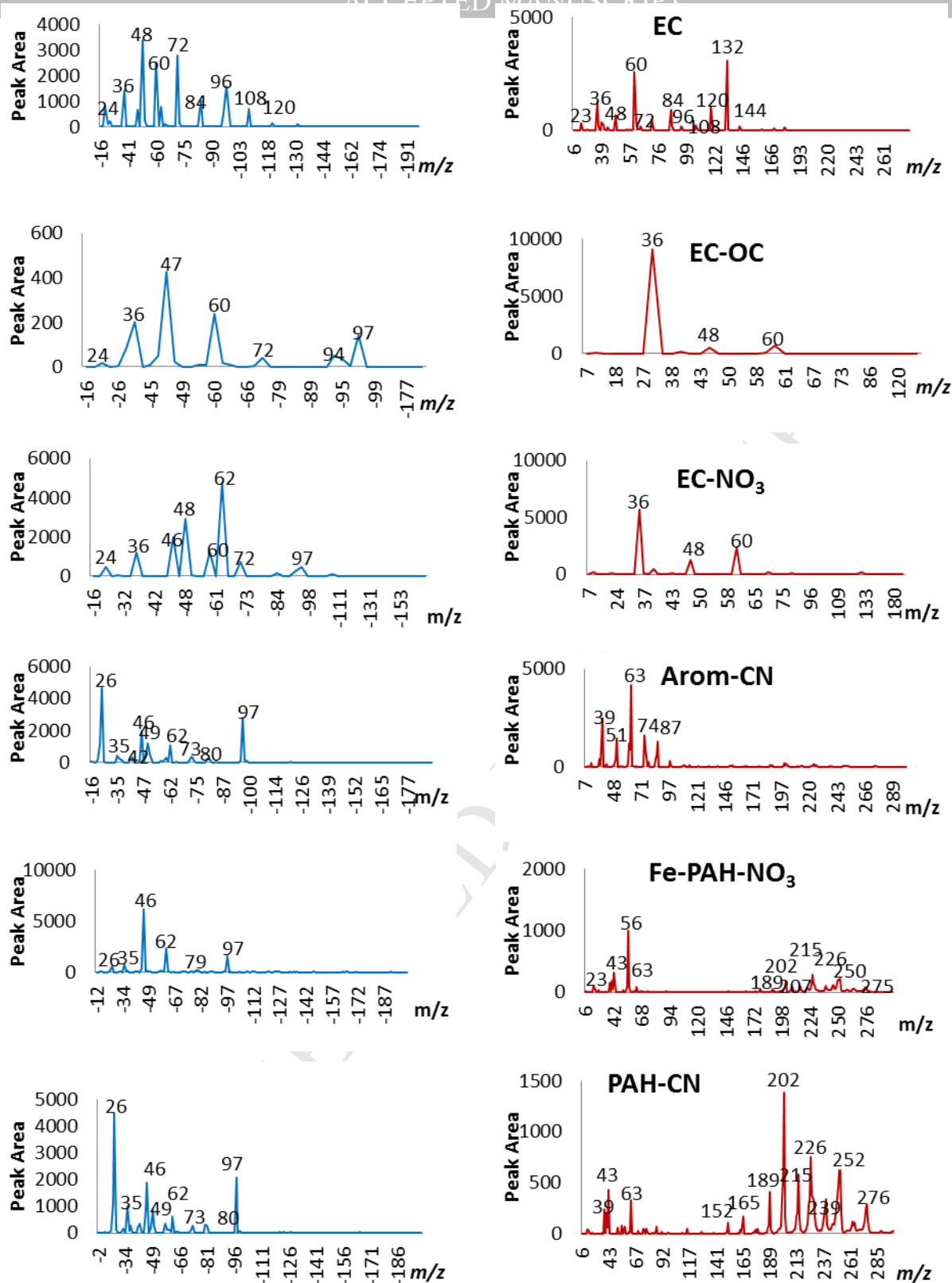
856

© Crown Copyright/database right 2011. An Ordnance Survey EDINA supplied service.

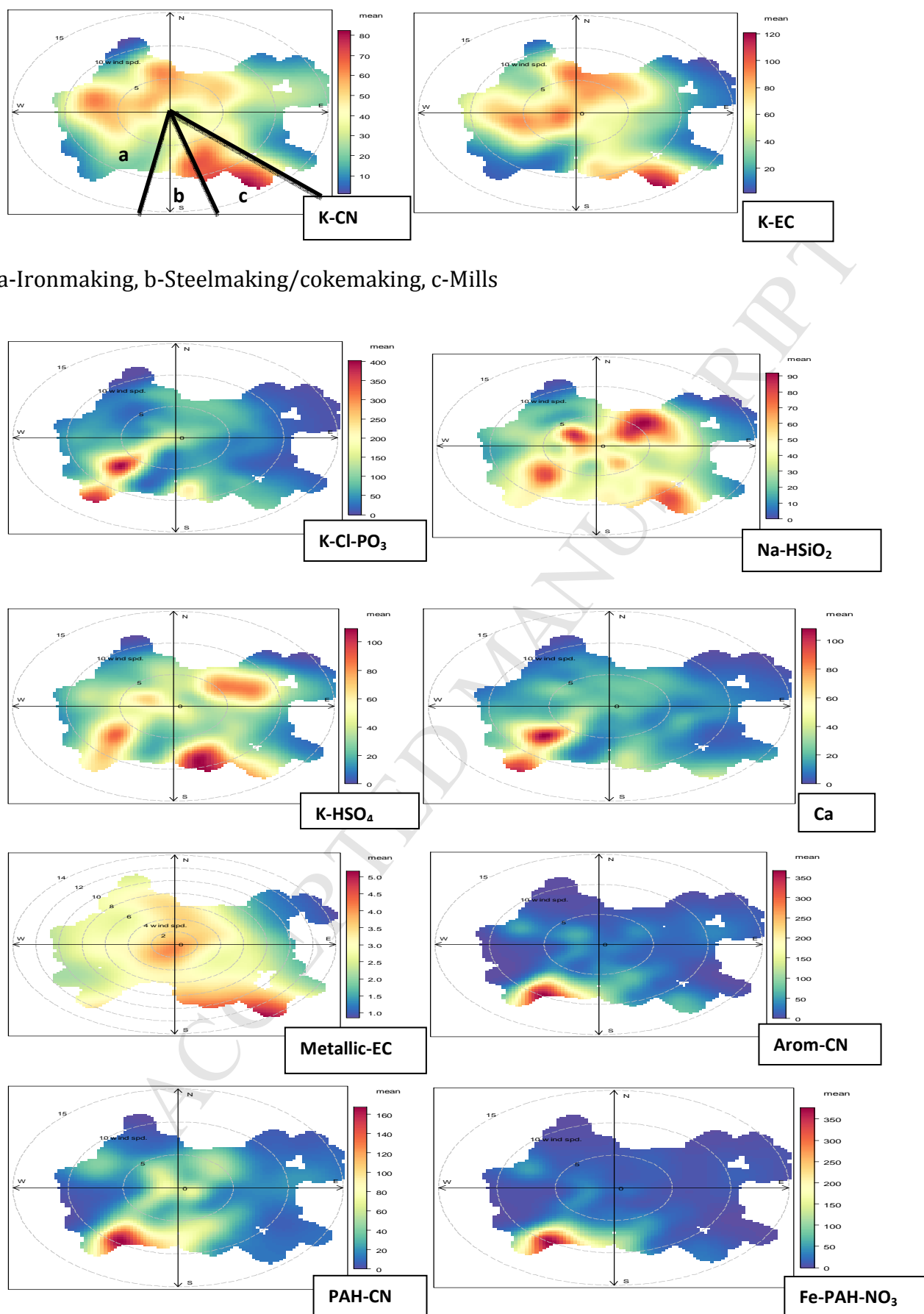
**Figure 1:** Port Talbot sampling station and the steelworks processing units



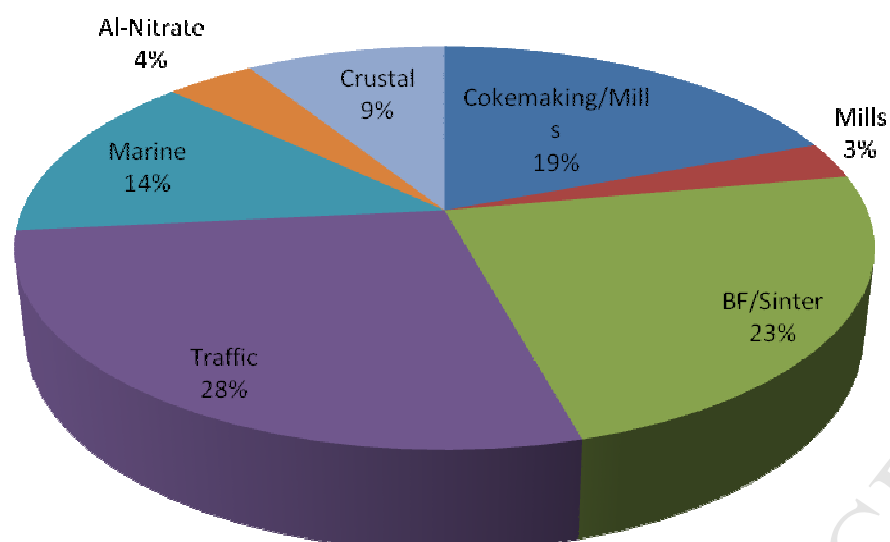




**Figure 2:** Mean mass spectra of particle clusters derived from the k-means clustering



**Figure 3:** Polar plots of steelworks particle clusters

**% Source Contributions**

**Figure 4:**Source contribution of particles derived from ATOFMS data



# **SOURCE APPORTIONMENT OF SINGLE PARTICLES SAMPLED AT THE INDUSTRIALLY POLLUTED TOWN OF PORT TALBOT, UNITED KINGDOM BY ATOFMS**

**Adewale M. Taiwo, Roy M. Harrison, David C.S. Beddows and  
Zongbo Shi**

## **HIGHLIGHTS**

- ATOFMS used to characterise over 500,000 single particles.
- Clustering revealed 17 distinct particle classes.
- Polar plots reveal source locations and identities.
- Estimate of steelworks contribution is compared to independent datasets.
- Cokemaking and blast furnaces contribute substantially to particle loadings.

**Supplementary Information****SOURCE APPORTIONMENT OF SINGLE PARTICLES  
SAMPLED AT THE INDUSTRIALLY POLLUTED TOWN OF  
PORT TALBOT, UNITED KINGDOM  
BY ATOFMS**

**Adewale M. Taiwo, Roy M. Harrison, David C.S. Beddows and  
Zongbo Shi**

**Table S1:** Abundance, size-association and notable mass spectral peaks of particle classes.

	Particle Classes	Clusters	Notable Peaks	Scaled ATOFMS aerodynamic diameter ( $\mu\text{m}$ )	Number of Particles	% of Particles
1	K-rich	K-CN	$m/z$ +23, +39, -26, -46, -62, -97	0.44	63459	11.4%
2		K-NO <sub>3</sub>	$m/z$ +39, -26, -46, -62, -97	0.37	92318	16.6%
3		K-EC	$m/z$ +23, +39, +60, -24, -26, -46, -48, -60, -62, -72, -84, -96, -108	0.42	39931	7.2%
4		K-Cl-PO <sub>3</sub>	$m/z$ +23, +39, -35, -46, -60, -62, -79, -96	0.49	61513	11.1%
5	Sea Salt	Na-NO <sub>3</sub>	$m/z$ +23, +39, -62, -46, -120, -147	1.05	29394	5.3%
6	Silica Dust	Na-HSiO <sub>2</sub>	$m/z$ +23, +39, -16, -26, -36, -46, -48, -61, -72, -79, -97, -142, -144	0.82	29137	5.2%
7	Sulphate	K-HSO <sub>4</sub>	$m/z$ +23, +39, +43, -26, -46, -62, -80, -97	0.37	29845	5.4%
8	Nitrate	AlO-NO <sub>3</sub>	$m/z$ +43, +137, -46, -62, 97	0.35	27358	4.9%
9	Ca-rich	Ca	$m/z$ +23, +40, -26, -36, -46, -47, -60, -62, -72, -79, -84, -97, -108	0.41	15303	2.8%
10	Carbonaceous	Mn-OC	$m/z$ +39, +55, -25	0.49	1742	0.3%
11		Metallic-EC	$m/z$ +23, +27, +41, +48, +56, +59, -24, -36, -48, -60, -72, -84, -96, -108	0.43	20339	3.7%
12		OC-EC	$m/z$ $\pm$ 36, $\pm$ 60, +48, -24, -47, -72, -94, -97	0.49	14619	2.6%
13		EC	$m/z$ $\pm$ 36, $\pm$ 48, $\pm$ 60, $\pm$ 72, $\pm$ 84, $\pm$ 96, $\pm$ 108, $\pm$ 120, +132, +144, -24	0.42	50657	9.1%
14		EC-NO <sub>3</sub>	$m/z$ $\pm$ 36, $\pm$ 48, $\pm$ 60, +39, -24, -46, -62, 97	0.51	10953	2.0%
15	Arom-PAH	Aromatic-CN	$m/z$ +39, +51, +63, +74, +87, +98, -26, -35, -46, -49, -62, -73, -97 (for $m/z$ >100, strong peaks were +188, +200, +202, +224, +250)	0.34	25242	4.5%
16		Fe-PAH-NO <sub>3</sub>	$m/z$ +56, -46, -62, -97, (for $m/z$ >100, strong peaks were +226, +250, +202, +250)	0.34	24980	4.5%
17		PAH-CN	$m/z$ +39, +43, +63, +152, +165, +189, +202, +215, +226, +239, +252, +276, -26, -35, -46, -48, -62, -73, -80, -97	0.35	18460	3.3%
Total					555,250	

**Table S2:** Particle types of Na-NO<sub>3</sub>, Al-nitrate, EC, OC-EC and OC-NO<sub>3</sub> during Port Talbot campaign

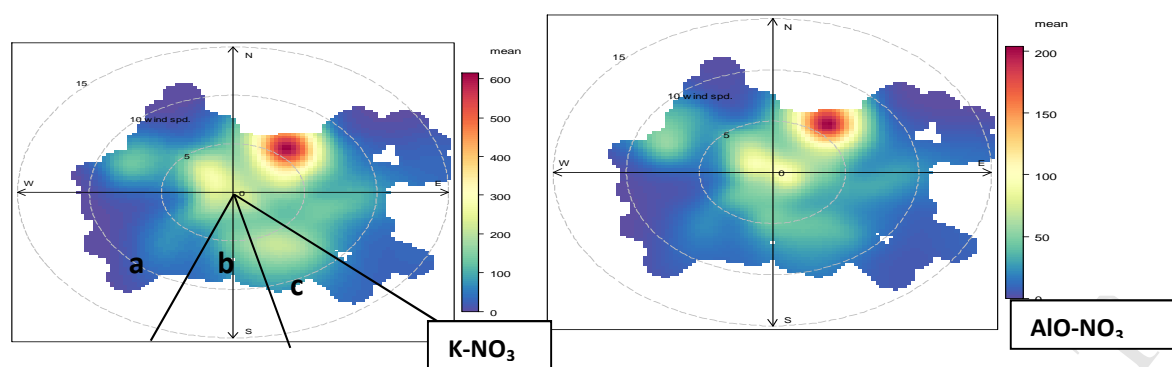
<p><b><i>The EC-OC particle</i></b></p> <p>Halogenated carbon has proved very difficult to observe in the negative spectrum and has been rarely observed in the positive spectrum (Silva and Prather, 2000). EC-OC exhibits a closer temporal relationship with metallic-EC (<math>r^2=0.80</math>) than any other carbonaceous particle class suggesting a common emission source. The EC-OC class shows a relatively weak association with the OC particle class (<math>r^2 = 0.22</math>) and a moderate relationship with EC-NO<sub>3</sub> (<math>r^2 = 0.33</math>). The polar plot is very similar to that of the EC class, and is strongly suggestive of a traffic source.</p>
<p><b><i>The Aromatic-CN particle</i></b></p> <p>Traces of PAH could be seen in this cluster at <math>m/z &gt; 100</math>. The <math>m/z +39</math>, <math>+51</math> and <math>+63</math> might also suggest the presence of <math>[K]^+</math>, <math>[V]^+</math> and <math>[Cu]^+</math>. The polar plot of this particle shows a clear steelworks emission from the blast furnace (BF) plant (<math>190-270^\circ</math>) and possible contributions from the cokemaking and basic oxygen furnace steelmaking (BOS) sections (<math>170-190^\circ</math>, Table 1). The presence of V might be indicative of an emission from shipping in the docks area.</p>
<p><b><i>Aged sea salt particles</i></b></p> <p>The strong nitrate and weak chloride peaks are reflective of considerable aging of the particle type. The chloride depletion in sea salt calculated from MOUDI samples (Gard et al., 1998; Taiwo et al., 2014) was 70%, supporting this interpretation. The spectral characteristics displayed by this cluster are related to features of fresh and aged salts described by Dall'Osto et al. (2004). However, the polar plot (Figure S1) indicates a range of wind directions and suggests that the particle is mainly of aged sea salt and may have been long-range transported.</p>
<p><b><i>Al-Nitrate (AlO-NO<sub>3</sub>) particle type</i></b></p> <p>Barium and aluminium could be associated with traffic emissions from brake wear and dust resuspension respectively (Gietl et al., 2010; Harrison et al., 2012b). The small elevation in concentration of this cluster at the centre of the plot is often indicative of local traffic emissions (see</p>

below) (Figure S1). A higher concentration of these particles to the north-east suggests traffic emissions from the local major highways.  $\text{AlO-NO}_3$  particles show a strong temporal relationship ( $r^2=0.70$ ) with  $\text{K-NO}_3$  particles consistent with a common emission source, but its identity is unclear.

**Table S3:** Comparison among particle classes observed in Port Talbot from 2004-2012.

	Particle Type	Smith, 2007	Dall'Osto et al., 2008*	Dall'Osto et al., 2012*	This Study
1	K-CN	X	✓	X	✓
2	K-NO <sub>3</sub>	✓	✓	X	✓
3	K-EC	X	X	X	✓
4	K-Cl-PO <sub>3</sub>	X	✓	X	✓
5	Na-NO <sub>3</sub>	✓	X	X	✓
6	Na-HSiO <sub>2</sub>	✓	X	X	✓
7	K-HSO <sub>4</sub>	✓	✓	✓	✓
8	AlO-NO <sub>3</sub>	X	X	X	✓
9	Ca	✓	X	X	✓
10	Mn-OC	X	X	X	✓
11	Metallic-EC	X	X	X	✓
12	EC-OC	✓	X	✓	✓
13	EC	✓	X	X	✓
14	EC-NO <sub>3</sub>	✓	X	X	✓
15	Aromatic-CN	✓	✓	✓	✓
16	Fe-PAH-NO <sub>3</sub>	✓	✓	✓	✓
17	PAH-CN	✓	✓	✓	✓
18	S	X	X	✓	X
19	HOC-Cl	X	X	✓	X
20	Zn	X	✓	X	X
21	Pb	✓	✓	X	X
22	Ni	X	✓	X	X
23	FeP	✓	✓	X	X
24	Amine	✓	X	X	X
25	Be-Sea Salt	✓	X	X	X
26	Mg Dust	✓	X	X	X

\* These papers are complementary as they report the metallic (2008) and non-metallic (2012) constituents respectively.



a-Ironmaking, b-Steelmaking/cokemaking, c-Mills

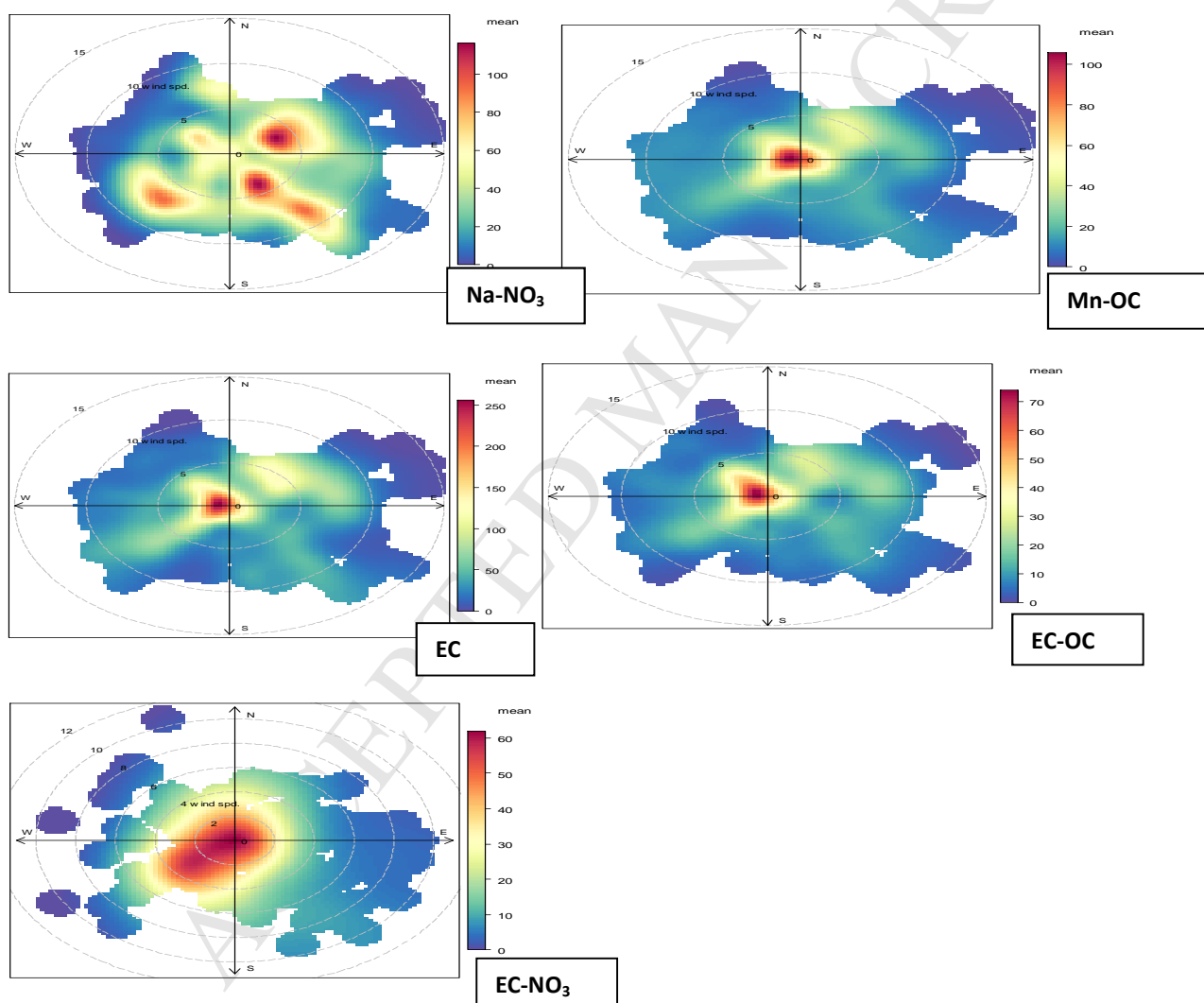


**Figure S1:** Polar plots of particle clusters



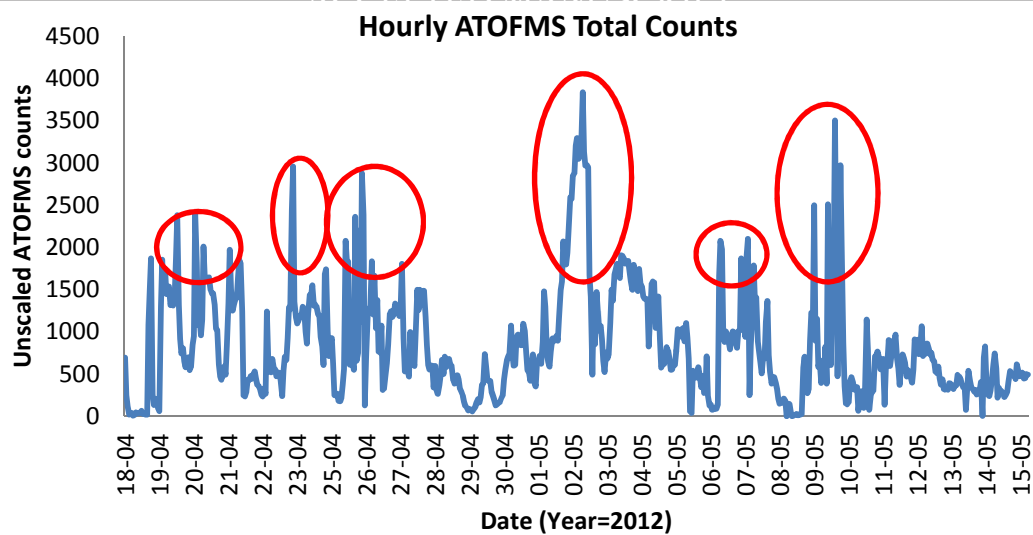


**Figure S2:** ATOFMS total particle number concentration [Red circles indicate the periods with elevated particle counts ( $> 2000/\text{hr}$ )].

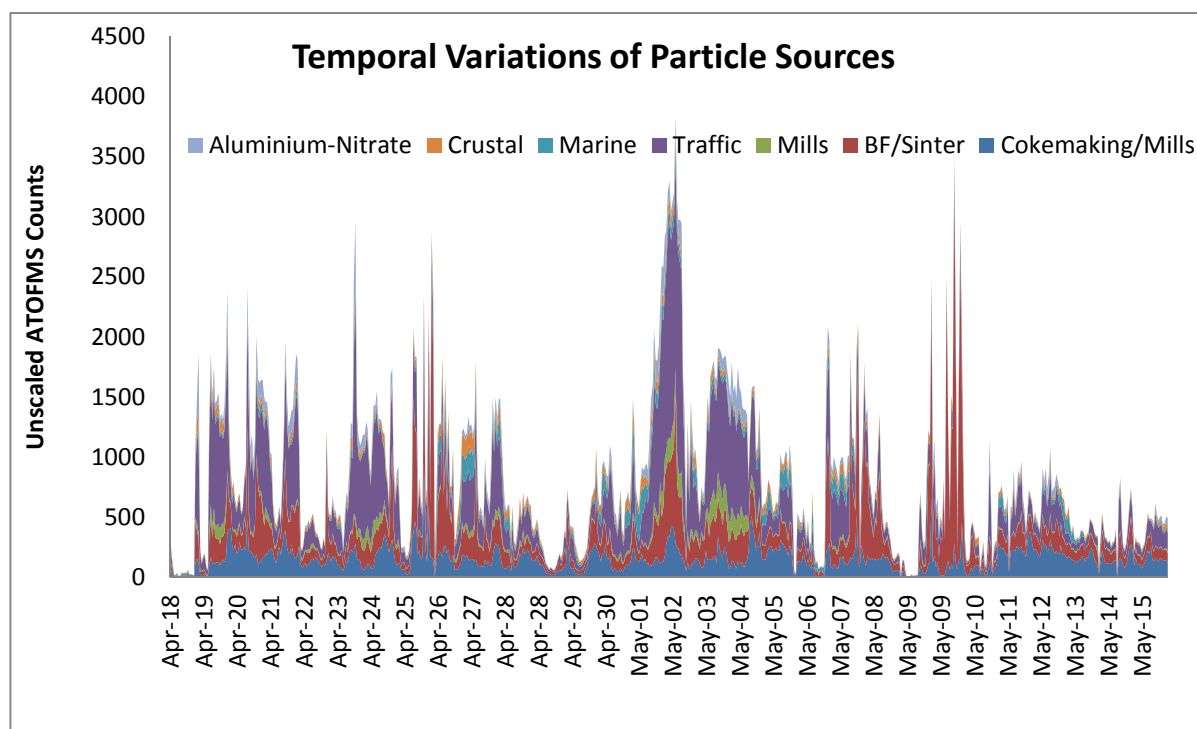


**Figure S3:** Temporal variations of hourly counts of particle classes.

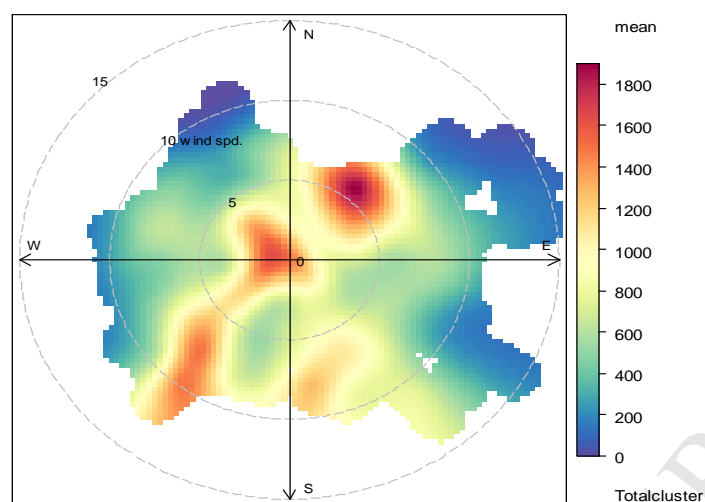


**Figure S4:** Polar plot of ATOFMS total particle counts

## REFERENCES

Dall'Osto, M., Beddows, D.C.S., Kinnersley, R.P., Harrison, R.M., Donovan, R.J., Heal, M.R. and 2004. Characterization of individual airborne particles by using aerosol time-of-flight mass spectrometry at Mace Head, Ireland. *J. Geophys. Res.*, 109 (D21), D21302.

Gard, E.E., Kleeman, M.J., Gross, D.S., Hughes, L.S., Allen, J.O., Morrical, B.D., Fergenson, D.P., Dienes, T., Galli, M.E., Johnson, R.J., Cass, G.R. and Prather, K.A., 1998. Direct observation of heterogeneous chemistry in the atmosphere. *Science*, 279, 1184-1187.

Silva, P.J. and Prather, K.A., 2000. Interpretation of mass spectra from organic compounds in aerosol time-of-flight mass spectrometry. *Anal. Chem.*, 72, 3553-3562.

Taiwo, A.M., Beddows, D.C.S., Shi, Z. and Harrison, R.M., 2014. Mass and number size distributions of particulate matter components: Comparison of an industrial site and an urban background site. *Sci. Tot. Environ.*, 475, 29-38.